Integrating multiple omics to identify common and specific molecular changes occurring in Arabidopsis under chronic nitrate and sulfate limitations

Jie Luo, Marien Havé, Gilles Clement, Frederique Tellier, Thierry Balliau, Alexandra Launay-Avon, Florence Guerard, Michel Zivy, Céline Masclaux-Daubresse

Integrating multiple omics to dissect the common and specific molecular changes occurring in *Arabidopsis thaliana* (L.) under nitrate and sulfate chronic limitations

Jie Luo[1,2,*] Marien Havé[1], Gilles Clément[1], Frédérique Tellier[1], Thierry Balliau[3], Alexandra Launay-Avon[4,5], Florence Guérard[4,5], Michel Zivy[3] and Céline Masclaux-Daubresse[1,*]

[1] Institut Jean-Pierre Bourgin, INRAE, AgroParisTech, Université Paris-Saclay, 78000, Versailles, France.

[2] College of Horticulture and Forestry Sciences, Hubei Engineering Technology Research Center for Forestry Information, Huazhong Agricultural University, Wuhan 430070, China.

[3] UMR GQE- le Moulon, INRAE, Université Paris-Sud, CNRS, AgroParisTech, Université Paris-Saclay, 91190, Gif-sur-Yvette, France

[4] Université Paris-Saclay, CNRS, INRAE, Univ Evry, Institute of Plant Sciences Paris-Saclay (IPS2), 91405, Orsay, France.

[5] Université de Paris, CNRS, INRAE, Institute of Plant Sciences Paris-Saclay (IPS2), 91405, Orsay, France

Corresponding authors (*):

Céline Masclaux-Daubresse: celine.masclaux-daubresse@inrae.fr, phone: +33 130833088

Jie Luo: jie.luo@vip.163.com

Running title: Omics of nitrate and sulfate chronic limitation

ORCID numbers:

Jie Luo: 0000-0003-1495-8239

Marien Havé: 0000-0002-2234-7043

Gilles Clément: 0000-0001-9899-2738

Frédérique Tellier: none

Thierry Balliau: 0000-0002-8172-1605

Alexandra Launay-Avon: 0000-0002-1993-313X

Florence Guérard: none

Michel Zivy: 0000-0002-9814-3792

Céline Masclaux-Daubresse: 0000-0003-0719-9350

Highlight

Multiomics study reveals common and specific effects of chronic nitrate or sulfate limitations, and enlighten interconnections and strategies of plant adaptation through the modulation of fundamental cell functions and metabolism.

Abstract

Plants, which have fundamental dependence on nitrogen and sulfur, have to cope with chronic limitations when fertilizers are not provided. Our study aimed at characterizing the metabolomic, proteomic and transcriptomic changes occurring in Arabidopsis leaves under chronic nitrate (Low-N) and chronic sulfate (Low-S) limitations in order to compare Low-S and Low-N effects and enlighten interconnections and strategies of plant adaptation.

Metabolite profiling globally revealed an opposite effect of Low-S and Low-N on carbohydrate and amino acid accumulations. Proteomic data showed by contrast that both Low-N and Low-S resulted in the exacerbation of catabolic processes, stimulation of mitochondrial and cytosolic metabolisms and decrease of chloroplast metabolism. The lower abundances of ribosomal proteins and translation factors under Low-N and Low-S attested from growth limitation. At transcript level, the major and specific effect of Low-N was the enhancement of plant defence and immunity genes. The main effect of chronic Low-S was the decrease of transcripts involved in cell division, DNA replication and cytoskeleton and the increase of autophagy gene expressions. This was consistent with a role of the Target-of-Rapamycin kinase in the control of plant metabolism and cell growth and division under chronic Low-S. In addition, Low-S decreased the expression of several NLP transcription factors, which are master actors of nitrate sensing. Finally, both transcriptome and proteome revealed the effect of Low-S on the repression of glucosinolate synthesis, and the effect of Low-N on the exacerbation of glucosinolate degradation. This showed the importance of glucosinolate as buffering molecules for N and S management.

Introduction

Plants have a fundamental dependence on inorganic nitrogen. As soil availabilities in nitrogen are generally poor, hundred million metric tonnes of nitrogenous fertilizers are added in the fields worldwide annually (Robertson & Vitousek, 2009). The preferred form in which N is taken up by plants is usually nitrate (NO_3^-). Some plants adapted to low pH and reducing soils like rice and plants from mature forests or arctic tundra tend to take up ammonium or amino acids. Nitrate uptake occurs at the root level and two nitrate transport systems from the NRT1 (LATS; low affinity transporters) and NRT2 (HATs; high affinity transporters) gene families coexist to act coordinately to take up nitrate from the soil, and distribute it within the whole plant and in the different cell compartments (Masclaux-Daubresse *et al.*, 2010; Tegeder & Masclaux-Daubresse, 2017). Nitrate reduction is catalysed by nitrate reductase (NR) in the cytoplasm of root and shoot cells, and the reduction of the nitrite produced is catalysed by nitrite reductase (NiR) in plastids and chloroplasts (Meyer *et al.*, 2005). NR is a homodimer. Each NR monomer

is associated to three prosthetic groups: flavin adenine dinucleotide (FAD), a heme, and a molybdenum cofactor (MoCo). The NiR protein is trimeric and contains siroheme and [4Fe-4S] prosthetic groups. The ammonium, originating from nitrate reduction is mainly assimilated in the plastid/chloroplast by the so-called GS2/GOGAT cycle (Masclaux-Daubresse *et al.*, 2010) and also, especially in the roots, by the cytosolic GS1 isoforms (Lothier *et al.*, 2011). Glutamine synthetases (GS) fixe ammonium on a glutamate molecule to form glutamine. Glutamine reacts subsequently with 2-oxoglutarate to form two molecules of glutamate; this step being catalysed by the glutamine 2-oxoglutarate amino transferase (or glutamate synthase, GOGAT; (Suzuki & Knaff, 2005). Glutamate and glutamine are then interconverted to form all the other amino acids. When plants are starved or ageing, they undergo nutrient remobilization from their leaves to support the growth of sink organs and fulfil storage compartments. N recycling and mobilization involves autophagy, proteases and enzymes in charge of the interconversion of amino acids for phloem loading and transfer throughout the plant (Have *et al.*, 2017; Tegeder & Masclaux-Daubresse, 2017).

Like nitrogen, sulfur (S) is an essential element for plant growth. It is an important constituent of S-containing amino acid (methionine and cysteine) and then for protein synthesis. It is also necessary in several S-secondary metabolisms (glucosinolates, glutathione) important for plant defence and redox homeostasis (Chan *et al.*, 2019). Sulphur deficiency in crops had become an agricultural concern since several decades due to the decrease of S deposition and of atmospheric sulphur dioxide emissions by industry. The S fertilization in crops is now considered in agriculture (McNeill *et al.*, 2005; Courbet *et al.*, 2019). S limitation can severely impact seed yield and quality in many species (Gironde *et al.*, 2014; Dai *et al.*, 2015; Postles *et al.*, 2016). Plants take up sulfur from the soil as sulfate (SO_4^{2-}). Both low-affinity and high-affinity sulfate transporters (SULTR) control the uptake and the flux of sulfate in the plant and in the different subcellular compartments (Takahashi, 2019). In a plant cell, sulfate is reduced to sulfite by the successive contribution of the ATP sulfurylase and adenosine phosphosulfate reductase (APR). The sulfite reductase (SiR) located in the plastids is responsible for the reduction of SO_2^- to S^{2-} (sulfide) (Kopriva, 2006). The sulfide is then assimilated into cysteine by the O-acetylserine (thiol)lyase (OASTL).

Nitrogen and sulfur nutritions and metabolisms are strongly coordinated as both are needed for protein synthesis and as the two major enzymes NiR and SiR share the same siroheme and [4Fe- 4S] prosthetic groups (Garai & Tripathy, 2018). Sulfur deficiency was shown to inhibit nitrate uptake and reduction, and nitrate deficiency inhibits sulfate uptake and reduction rate (Jobe *et al.*, 2019). Reduced N forms as ammonium and amino acids positively regulate APR, while cysteine stimulates NR (Kopriva & Rennenberg, 2004).

Several studies have investigated metabolomic and transcriptomic changes in response to low nitrate nutrition (Scheible *et al.*, 2004; Krapp *et al.*, 2011; Engelsberger & Schulze, 2012; Ristova *et al.*, 2016). These studies usually applied short term starvation treatments (hours), some resupplied nitrate, and they all were mainly interested in finding components involved in nitrate signalling. The global transcription profiling performed by Bi *et al.* (2007) was different and considered transcriptomic changes in Arabidopsis rosettes under mild or severe chronic N limitations. This allowed them to depict changes in N-uptake and N-assimilation, characterize the major metabolic changes and identify genes strongly

modified by chronic N-limitation. By contrast with transcriptome and metabolome, studies dealing with proteomic changes under N starvation are scarce and there is no proteomic study on chronic N limitation in plant.

Watanabe & Hoefgen (2019) recently published a survey of the transcriptomic, metabolomic and proteomic studies on the effect of S-starvation, performed in several plant species. Their review shows how transcriptomes revealed several transcription factors associated to changes in the availability of S, especially many involved in the control of glucosinolate metabolism. Proteomic studies on S-deprived plants were less numerous and mainly focused on seeds (Higashi *et al.*, 2006; D'Hooghe *et al.*, 2014; Bonnot *et al.*, 2020).

Our study aims at characterizing the metabolomic, proteomic and transcriptomic changes occurring in Arabidopsis leaves under chronic nitrate or sulfate starvations. Our results show how nitrate- and sulfate- limitations influence plant metabolism and cellular processes in different or similar ways, and provide comprehensive picture of interconnections between N and S metabolisms.

Material and methods

Plant material and growth conditions

The seeds of *Arabidopsis thaliana* (L.) Columbia Col-0 accession were sown in pots containing fine sand, and cultivated for 60 days after sowing according to Havé *et al.* (2019), in short days (8 h light, 160 µmol photon $.m^{-2}.s^{-1}$). Plants were grown under control (Ctrl; 10 mM NO_3^- and 0.266 mM SO_4^{2-}), low nitrate (Low-N; 2 mM NO_3^- and 0.266 mM SO_4^{2-}) or low sulphur (Low-S; 10 mM NO_3^- and 0.016 mM SO_4^{2-}), see Table S1 for details. For the control and Low-S conditions, each pot contained one plant; under Low-N conditions there were six plants per pot. These adequate growth conditions for trial of nitrogen and sulfur limitation effects on Arabidopsis plants had been established by Loudet *et al.* (2003) and Lornac *et al.* (2020). Whole rosettes were harvested 60 days after sowing (DAS). Four independent plant replicates were obtained. For control and Low-S conditions, each biological replicate contained 4 rosettes. For Low-N conditions, biological replicates contained 24 rosettes each. Harvests were performed between 10:00 and 11:00 AM, and samples were stored at -80°C for further experiments. Plant culture was repeated 3 times, providing samples from 3 independent experiments.

Shotgun proteomic analysis

Leaf total proteins extraction, trypsin digestion, LC-MS/MS analysis and protein identification were performed according to Havé *et al.* (2018) on three independent biological replicates (see supplementary information) at the PAPSSO platform (INRA, Le Moulon, Gif sur Yvette). Peptide quantification by peak area integration on eXtracted ion chromatogram (XICs) was performed using the MassChroQ software (pappso.inra.fr/bioinfo/masschroq/; Valot *et al.*, 2011) according to Balliau *et al.* (2018). Normalization was performed taking into account peptide retention time as described in Lyutvinskiy *et al.* (2013). Proteins were then quantified based on peptide intensities by filtering for protein-specific peptides present in at least 90% of the samples and showing a correlation ($r > 0.6$) with the other peptides of the same protein. Relative protein abundances were then calculated and defined

as the sum of XICs intensities of selected peptides. When the peptides of a protein were not present or not reproducibly observed in one or several conditions, spectral counting (SC) was used in place of XICs analysis. Only proteins that produced at least four protein-specific spectra in at least one sample were considered for spectral counting quantification. We considered that proteins which did not match this threshold were of too low abundance to be reliably quantified.

RNA extraction and RNA-Seq.

RNA were extracted from the same samples as proteins. Nine samples were produced with 3 independent biological replicates. Note that RNA were extracted from the same samples as proteins and metabolites. Total RNA was extracted from rosettes using TRIzol protocol (Invitrogen®, Thermo Fisher Scientific, California, U.S.A.) and purification by using RNeasy MinElute Cleanup Kit (Qiagen, Hilden, Germany). For each biological repetition, RNA samples were obtained by pooling RNAs from more than 4 plants. Sequencing technology used was an Illumina NexSeq500 (IPS2 POPS platform). RNA-seq libraries were performed by TruSeq Stranded mRNA SamplePrep protocol (Illumina®, California, U.S.A.). The RNA-seq samples have been sequenced in single-end (SE), stranded with a sizing of 260bp and a read length of 75 bases, lane repartition and barcoding giving approximately 22 millions of SE reads by sample. The RNAseq data have been submitted to the Sequence Read Archive (SRA) database under BioProject, the ID is PRJNA622692.

Metabolome analyses and data mining

Profiling of small metabolites (sugars, amino acids, ketonic acids) was performed using GC-MS according to Masclaux-Daubresse *et al.* (2014). Lipid analyses were performed using LC-MS and GC-MS according to Havé *et al.* (2019). ATP, ADP, NAD(P)(H), glutathione and ornithine contents were measured using LC-TOF according to Guerard *et al.* (2011). All these experiments were performed on 3-4 biological replicates.

Sulfate and nitrate determinations

Nitrate and sulfate were extracted from lyophilized material (50 mg DW in 1 mL H_2O) by shaking for 4 hours. After centrifugation (10 min, 12,000 g) supernatant was cleared by centrifugation after adding TCA 3M (10µL per mL). Nitrate was determined using the Cataldo et al. (1975) method. Sulfate was determined measuring turbidity with spectrometer at 600 nm in 96 wells microplate. For that 180 µL of cleared supernatant were added to 60 µL of HCl 0.5 N and mixed. Then, 60 µL of Barium buffer (BaCl2 40 µM; PEG 6000 150 mg/ mL; Na_2SO_4 0.1 mM) was added to develop turbidity. Standard curve was obtained by successive dilutions 0-50 mM of Na_2SO_4. Blank was water.

Bioinformatics analysis

For proteomic and metabolomic data, Student's t-test was used to compare the changes between nutrition treatments (Low-N and Low-S) and control condition. For proteome, *p*-value of t-test lower than 0.05 and FC above (or lower) than 1.2 (or -1.2) were applied as cut-off to select the differentially accumulated proteins (DAPs). For transcriptome analyses, each sample followed the same steps from trimming to count. RNA-Seq preprocessing includes trimming library adapters and performing quality controls. The raw data (fastq) were trimmed with Trimmomatic (Bolger *et al.*, 2014) tool for Phred Quality Score Qscore >20, read length >30 bases, and ribosome sequences were removed with tool

sortMeRNA (Kopylova *et al.*, 2012). The quality of clean data was checked with FastQC software. Then clean reads were mapped onto Arabidopsis thaliana genome (TAIR10) using "align" software in Subread (version 2.0.0) (Liao *et al.*, 2013). Counts for each gene were calculated using featureCounts software (Liao *et al.*, 2014) with Arabidopsis thaliana annotation version Araport11. The differentially expressed genes (DEGs) were computed in R with DESeq2 package (Love *et al.*, 2014). The fold change above 2 (or lower than -2) and FDR lower than 0.05 were considered as cut-off to select the significant genes. Functional information and cellular location for each protein (or gene) were analysed using MapMan (https://mapman.gabipd.org/) software and SUBA4 (http://suba.live/). Gene Ontology, AraCyc, Gene Family and KEGG analyses were conducted using VirtualPlant 1.3 (http://virtualplant.bio.nyu.edu/cgi-bin/vpweb/). The proteomic data have been submitted to http://moulon.inra.fr/protic/autoadapt_2015. The significances of intersections between DAPs and DEGs were determined by SuperExactTest package in R software (Wang *et al.,* 2015).

Results and Discussion

Metabolite profiling reveals specific changes in the rosette of plants submitted to chronic N- or S-limitations

Metabolite profiling using GC-MS identified 120 metabolites in the rosettes of Arabidopsis plants cultivated under control (Ctrl), low nitrate (Low-N) and low sulfate (Low-S) conditions for 60 days (Fig.S1). Among the detected metabolites, 54 showed significantly different concentrations in the rosettes of plants grown under N or S limitations by comparison to the Ctrl condition (Fig.1,2). The LC-MS lipid, cofactor, glutathione and nucleotide analyses also revealed significant differences between nutritive conditions (Fig.1,2). Measurement of nitrate and sulfate by spectrometry indicated that nitrate concentration was not modified under Low-S but decreased 3 times under Low-N, and that sulfate concentration was slightly but significantly increased under Low-N (1.5 fold) and sharply decreased under Low-S (12 fold).

Main changes in the rosettes of the N-limited plants (Fig.1) were a strong increase of carbohydrate concentrations as sugars (minor CHO and hexoses), lipids (MGDG, DGDG and GIPC) and of ketonic acids involved in the TCA cycle (malate, citrate, aconitate and 2-oxoglutarate). ADP concentrations were higher and ATP concentrations lower under Low-N conditions. As a result, the ATP/ADP ratio was lower under Low-N than in control condition. In the category of CHO metabolism, mannose, melibiose, galactose, raffinose, galactinol, gluconate and galactonate were increased; only erythritol was depleted under Low-N. Metabolites as dehydroascorbate and α-tocopherol were increased while reduced glutathione (GSH) concentrations were decreased and oxidized glutathione (GSSG) increased suggesting higher oxidative stress under Low-N than in Ctrl. Individual amino acid concentrations did not change in a similar way. Glutamate and aspartate that are directly connected to the Krebs cycle were more abundant under Low-N, while the concentrations of the amino acids usually considered as

N-storage molecules like glutamine and proline were lower under Low-N. Ornithine that is connected to the proline pathway was accordingly less abundant in the Low-N rosettes, as well as the putrescine and spermidine polyamines. The amino acids belonging to the glycine/serine pathway were also less abundant under Low-N as well as threonine and alanine. Surprisingly methionine and tryptophan which are two precursors of glucosinolates were more abundant under Low-N (Aarabi *et al.*, 2016).

Metabolite changes in the rosettes of plant grown under Low-S were less numerous, compared to Low-N (Fig.2). There was almost no change in minor CHO, except a decrease of mannose. Interestingly, while glucose and fructose were less abundant under Low-S, their phosphorylated forms glucose 6-P and fructose 6-P were more abundant. Similarly, the concentration of myo-inositol was lower under Low-S than in Ctrl condition, while concentration of myo-inositol-1-P was higher under Low-S. It can be noticed that phosphate content was also higher under Low-S. Glycine, serine, alanine, threonine, leucine and aspartate concentrations were higher under Low-S than under Ctrl condition, which was globally an opposite trend as under Low-N condition, except in the case of aspartate and leucine. Among amino acids, only ornithine and cysteine were less abundant under Low-S. GSH and GSSG were less abundant under Low-S, which makes sense knowing that cysteine is needed for glutathione synthesis. Methionine was not modified by Low-S. Lipids whose synthesis depends on acetyl-CoA and then on sulfur metabolism, were less abundant under Low-S than under Ctrl, which was the opposite trend as compared to the Low-N effect. Although GSH and GSSG were less abundant under Low-S than in Ctrl condition, the slightly higher GSH/GSSG ratio and the higher α-tocopherol and γ-tocopherol concentrations suggested higher oxidative stress in the Low-S rosette leaves. As tocopherols are mostly associated to chloroplast membranes and lipid bodies, this is consistent with the lower concentrations of MGDG and DGDG lipids observed under Low-S that suggest chloroplast defects. All the nucleotides detected were less abundant under Low-S.

The leaf proteome is modified when nitrate or sulfate is limiting

A total of 2334 proteins were identified and quantified by XIC from the proteome analyses of the rosettes of the Low-N, Low-S and Ctrl plants. Among them, proteins significantly differentially accumulated (DAPs; differentially accumulated proteins) under Low-N or Low-S relative to Ctrl were identified. There were 965 DAPs for Low-N and 676 DAPs for Low-S. (Table S2, Fig.3A). Under Low-N, 645 were more abundant and 320 less abundant than in Ctrl condition. Under Low-S, 350 DAPs were more abundant and 326 less abundant. The intersection between Low-N and Low-S changes includes 210 and 140 proteins that were respectively more and less abundant compared to Ctrl condition in both Low-N and Low-S conditions. This intersection represented 27% of the DAPs (Fig.3A). The predicted cellular location of DAPs was mostly similar under Low-N and Low-S conditions (Fig.3B). For instance, DAPs with higher abundance under Low-N or Low-S were mainly predicted in mitochondria, extracellular and cytosolic spaces. The DAPs identified as less abundant under Low-N or Low-S were mainly predicted in plastid and cytosol (Fig.3B).

Modification of leaf proteome under Low-N reflects senescence-like catabolic events

GO term enrichment for “biological process” (BP) and “molecular function” (MF) were also examined using VirtualPlant 1.3, and *P*-value cut off was 0.01. The analyses were done separately on the lists of the more abundant (UP) and on the less abundant (DOWN) DAPs found in Low-N *vs.* Ctrl (Tab.S3). Enrichment in BP GO terms indicated that for both the UP and DOWN DAPs, the “metabolic processes” and “response to stimuli” categories were enriched. The MF GO term analysis of the UP DAPs grouped oxido-reduction activities, peptidase and hydrolase catalytic activities, antioxidant activities and ion binding activities. The DOWN DAPs were related to N metabolic processes, including cellular N compound metabolism, tetrapyrrole metabolism and amino acid metabolism. The DOWN DAPs under Low-N were enriched in catabolic activities related to lyases, especially those involved in the bindings of N to metals and C to C. Structural molecules were also more represented in the DOWN DAPs.

Significant enrichments of DAPs list in terms from the Gene Family, AraCyc pathway and KEGG classifications were also analyzed using the VirtualPlant 1.3 BioMaps tool (http://virtualplant.bio.nyu.edu/cgi-bin/vpweb/) applying a *P*-value cut off of 0.05 (Tab.S3, Fig.3C). The AraCyc pathways, KEGG pathway and GENE Family terms confirmed that the UP DAPs with higher protein level under Low-N were involved in protein, amino acid, lipid and cell wall degradations, in the major and minor carbohydrate (major CHO and minor CHO) metabolisms, in redox and antioxidant activities, and in the energy metabolisms related to the mitochondria tricarboxylic acid cycle (TCA), mitochondria electron transport and to the cytosolic pentose phosphate pathway (Tab.S3). DAPs that were less abundant under Low-N were mostly involved in photosynthesis and photorespiration, in tetrapyrrole synthesis, plastid amino acid synthesis, cell wall synthesis, chloroplast fatty acid synthesis, protein translation and synthesis, and in water transport (aquaporins). The nature of the UP and DOWN DAPs under Low-N then reflected the exacerbation of catabolic pathways and the attenuation of chloroplast functions for energy production paralleled by an increase of the mitochondria and cytosolic energy pathways. The metabolic picture reflected by the term analyses of the Low-N DAPs was then in good accordance with the metabolite changes presented above and that showed higher minor CHO and sugar contents, higher TCA ketonic acid contents and depletion of many amino acids and especially N-rich amino acids as glutamine and proline.

The metabolic picture provided by the Low-N DAPs then reveals strong resemblance with metabolite changes that have been described for leaf senescence in the literature (Watanabe *et al.*, 2013; Clément *et al.*, 2018; Avila-Ospina *et al.*, 2017). This feature is consistent with the fact that nitrate starvation/limitation has been described as master leaf-senescence triggering factor (Diaz *et al.*, 2008). Consistently, amongst the Low-N DAPs we observed the decrease of enzymes involved in the nitrate primary assimilation (GLU1 Fd-GOGAT; GLT1 NADH-GOGAT; NIA2 nitrate reductase) and the increase of enzymes involved in N-recycling and remobilization (GLN1;1 and GLN1;3 cytosolic glutamine synthetases; GDH1 glutamate dehydrogenase (Fig.4). Numerous enzymes involved in protein

degradation were also increases and amongst them several have been previously described as senescence-induced and N-remobilization actors like AALP (Arabidopsis aleurain-like protease), RD19A (responsive to dehydration 19) and RD21A (responsive to dehydration 19), (Desclos *et al.*, 2009; Have *et al.*, 2017; Pružinská *et al.*, 2017; Havé *et al.*, 2018; Fig.5A). Surprisingly, the papain-like cysteine protease SAG12 which is one of the most highly induced and accumulated during leaf senescence and nitrogen remobilization (Desclos *et al.*, 2009; James *et al.*, 2018) was not over-accumulated in our Low-N condition, but was less abundant under Low-N than in Ctrl (Fig.5A). All the CLP chloroplast proteases were less abundant in Low-N except CLPD (also named ERD1 or SAG15), which is known to be induced by leaf senescence. Several chloroplast proteases involved in the degradation of thylakoid proteins as DEG1 (Degradation of Periplasmic Proteins 1), DEG8 and FTSH8 (Filamentation Temperature Sensitive H 8) were also more abundant under Low-N which may be consistent with the lower level of chloroplast proteins and especially the lower abundance of chlorophyll-binding proteins. Accumulation of several of proteasome proteins was also observed, which could indicate both higher proteasome activity under Low-N and lower proteaphagy (Marshall *et al.*, 2015; Fig.5A).

Potential protein substrates for N-remobilization as ribosomal proteins (Fig.5B) and chloroplast proteins (Fig.6) were consistently less abundant under Low-N than in Ctrl condition. The lower abundance of chloroplast proteins involved in photosynthesis or photorespiration under Low-N confirmed senescence-like picture. However, the decrease in many chloroplastic ribosomal proteins was paralleled with decrease in several cytosolic ribosomal proteins, initiation factors, elongation factors and tRNA ligase, which showed that translation machinery was less active under Low-N than under Ctrl conditions. It is noticeable that although changes in protein and transcript levels were globally not well correlated (Tab.S2), the lower abundance of the DAPs related to chloroplast photosynthetic apparatus was accompanied by the decrease of their corresponding transcripts. This suggests that the lower levels of photosynthetic proteins under Low-N were not only due to extensive chloroplast degradation or turn over, but also to the down-regulations of these DAPs coding genes. It is known that during leaf senescence mitochondria stay active until late senescence and that energy metabolism is largely supported by cytosolic and mitochondria enzymes. Similarly, many enzymes related to neoglucogenesis, pentose phosphate pathway, glycolysis and TCA were more abundant under Low-N than in Ctrl condition (Fig.7).

Leaf proteome reveals strong inhibition of S-metabolism and increase of catabolic enzymes when sulfur supply is limiting

The enrichment in BP GO terms of the Low-S UP and DOWN DAPs indicates that the main changes were for “metabolic processes” and “response to stimuli”. The MF GO terms indicate that UP DAPs under Low-S are related to oxidoreduction activities and hydrolases/peptidase catalytic activities. For the DOWN DAPs the MF GO terms indicate that they are related to structural proteins, tetrapyrrole synthesis, lyase and ligase catalytic activities, and transporters. Several of these terms were shared by the Low-N DAPs.

The AraCyc, KEGG and Gene Family terms give a better idea of the modifications in the Low-S rosettes at the proteomic level (Tab.S4). DAPs with higher abundance under Low-S were related to fatty acid degradation. Accordingly, the amount of several lipids (MGDG monogalactosyldiacylglycérols, DGDG digalactosyldiacylglycérols, GIPC glycosyl-inositol-phospho-ceramides, PE phosphatidylethanolamine and PG phosphatidylglycerol) was lower in Low-S (Fig.2). The UP DAPs were also enriched in proteins involved in the degradation of amino acids, thymine and melibiose. However, this was not reflected by our metabolite profiling. Like under Low-N, several proteases were more abundant under Low-S, and higher accumulations of RD21A, RD19A and AALP were also observed (Fig.5A). Enrichment of the UP DAPs in proteins related jasmonate biosynthesis suggests an exacerbation of the response to stress under Low-S condition. The DAPs with lower abundance under Low-S presented enrichment in proteins involved in the translation machinery (ribosomal proteins and initiation factor; Fig.5BC), in photosynthesis and photorespiration (Fig.6), and in water transport (aquaporins, PIP, MIP, V-ATPases). This picture reflected many similarities in the pathways modified under Low-S and Low-N, even though the DAPs involved in these pathways were not always the same under Low-S and Low-N. Unsurprisingly, S metabolism including glucosinolate synthesis and glutathione S-transferase families were strongly impacted by Low-S condition (Tab.S4). The two ATP sulfiurylases ATPS1 (AT3G22890) and ATPS2 (AT1G19920) and the methionine synthase MS2 (AT3G03780) were less abundant under Low-S than in Ctrl condition (Tab.S2; Fig.8). Like for Low-N, changes at protein levels were poorly correlated with changes at transcript levels (Tab.S2), except in the case of the glucosinolate-related DAPs. Indeed, the lower abundance of glucosinolate-related DAPs under Low-S was paralleled by the lower abundance of their related transcripts.

Common proteome changes under low-N and low-S

Gene ontologies on DAPs show that there are several similar effects of the Low-N and Low-S growth conditions on rosette proteome (Tab.S3 and Tab.S4). We then analysed the 350 DAPs identified in both Low-N and Low-S conditions. Although this list (210 more abundant, 140 less abundant) was not large, significant terms were identified (Tab.S5; Fig.3C). The GO terms showed enrichments in the oxidoreduction and peptidases/hydrolases catalytic activities in the 210 UP DAPs, and enrichment in structural molecules and constituents of ribosomes in the 140 DOWN DAPs. The common effect of both Low-S and Low-N growth was also the exacerbation of the carbohydrate/starch degradation pathways and of the TCA energy metabolism, and enrichment of UP DAPs in proteins involved in the jasmonate synthesis. The DOWN DAPS were enriched in proteins involved in translation and protein synthesis (ribosomes, eukaryotic initiation factors), chloroplast metabolisms (photosynthesis, photorespiration), aquaporins and membrane ATPases, and in many steps of the lipid synthesis. Interestingly one transcription factor, Whirly1 appeared significantly reduced under both Low-N and Low-S. This Whirly1 transcription factor has been described as an important factor controlling chloroplast-cytosol signalling and leaf senescence onset in both Arabidopsis and barley (Lin *et al.*, 2019; Ren *et al.*, 2017; Swida-Barteczka *et al.*, 2018; Krupinska *et al.*, 2019). In barley, it was shown that Wirly1 functions in the control

of responses to N deficiency (Comadira *et al.*, 2015). Our result then suggest that Wirly1 could also control responses to S limitation.

Proteome changes highlight the cross-effects of nitrate and sulfate on the N and S metabolisms

It is known for long that nitrate availability can influence S uptake and metabolism as well as sulfate availability can influence N metabolism (Barney & Bush, 1985; Lee & Kang, 2005; Kopriva & Rennenberg, 2004; Kopriva, 2006). Both N and S are constituents of amino acids. Shortage of N and S sources may reduce amino acid biosynthesis, and further affects the protein translation (Speiser *et al.*, 2018). As said previously, Low-S leads to reduced abundance of ATPS1 and ATPS2; interestingly N deficiency also decreased ATPS2 (Fig.8A). Furthermore, sulfite reductase (SIR; AT5G04590) was accumulated in response to N limitation. N deficiency also led to increase the amounts of the two cysteine synthases (OASC, AT3G59760 and CYSC1, AT3G61440) and to the decrease of the plastid OASB cysteine synthase (AT2G43750) although the concentration of cysteine remained unchanged. By contrast, the lower abundance of the cystathionine gamma synthase CGS1 (also called CYS1 and MTO1 for METHIONINE OVERACCUMULATION 1; AT3G01120) may explain that methionine was more abundant under Low-N than under control condition (Hacham *et al.*, 2013); Fig.8A; Fig.2). In Fig.8B.C. we can see that Low-N and Low-S had different effects on the glutathione and glucosinolate pathways. Both glutathione and glucosinolates necessitate nitrogen and sulfur for their synthesis. Regarding the glutathione metabolism, enzymes involved in the pathway were mostly more abundant under Low-N than under Ctrl condition and at the reverse less abundant under Low-S relative to Ctrl. Main changes were observed for glutathione S-reductases and the UP DAPs under Low-N were mostly involved in the pathways mobilizing glutathione for the synthesis of glycine or glutamate. For instance, the GSH1, GPX1, DHAR3, as well as several enzymes that are involved in the conversion of GSH to R-S-glutathione were less abundant under Low-S. This might be due to the lower concentrations of GSH and GSSG available under Low-S. For glucosinolates, it is interesting to note that many of the enzymes involved in glucosinolate synthesis were less abundant under Low-S, while Low-N mainly increased the abundance of the enzymes involved in glucosinolate degradation. Such effect of Low-N could be part of the exacerbation of the response stress DAPs as mentioned above. As both glutathione and glucosinolate are N sources, all these features regarding glucosinolate and glutathione pathways are consistent with the exacerbation of N-recycling processes. Proteomic data also revealed the strong influence of Low-S on amino acid metabolism as shown in Fig.4, however effects of Low-S on individual amino acid pathways was mostly different from Low-N changes.

Integration of data reveals that changes at proteomic and transcriptomic levels poorly match

Transcriptome was performed using RNAseq and significantly differentially expressed genes (DEGs) were identified by DESeq2 package (Love *et al.*, 2014). There was 2447 DEGs under Low-N and 5136 DEGs under Low-S (Fig.9; Fig.S2A; Tab.S6A,B,C). Then, proteome analysis revealed approximately twice more DAPs under Low-N than under Low-S, RNAseq analysis identified was twice more DEGs under Low-S than under Low-N. Such discrepancy reflects the poor correlation between protein accumulation/deletion and transcript accumulation/depletion already mentioned above, and illustrated in Fig.S2B-D. As such, only 102 and 53 gene accessions changed at both transcriptomic and proteomic levels under Low-N and Low-S respectively (Fig.S2B.C.). Only 20 of such accessions were found under both the Low-N and Low-S conditions (Fig.S2D).

Low-N transcriptomic changes reveals enhancement of defense genes

Under Low-N, many DEGs were unsurprisingly related to nitrogen metabolism. Several nitrate-responding transcription factors (TF) were up-regulated in the Low-N rosettes compared to Ctrl, as the *LBD39* (At4g37540) and *LBD38* (AT3G49940) LOB DOMAIN CONTAINING PROTEINS and the *NLP3* (AT4G38340) and *NLP9* (AT3G59580) NIN-like RWP-RK domain-containing protein. The *HHO3* (AT1G25550) and *HHO2* (AT1G68670) nitrate-inducible HRS1 homologues that may play a role in a pathway at the intersection of N and P signaling were down-regulated (Medici *et al.*, 2019; Vidal *et al.*, 2020). Accordingly, we found under Low-N higher expression of the *AtNRT2.5* nitrate transporter (AT1G12940) which is a well-known marker of nitrate starvation (Lezhneva *et al.*, 2014). At the reverse, the *CLC-A* and *CLC-B* chloride channels, that function as nitrate/proton exchangers at the tonoplast, were down regulated (De Angeli *et al.*, 2006). The *GLN1;1* (AT5G37600) and *GLN1;4* (AT5G16570) cytosolic glutamine synthetase genes involved in N-remobilization were up-regulated as the expression of the genes coding the master enzymes in charge of the nitrate primary assimilation - i.e. the chloroplastic glutamine synthetase *GS2* (AT5G35630), the *GLU1* Fd-dependent glutamate synthase (AT5G04140), the NIR1 nitrite reductase (AT2G15620) and the *NIA1* nitrate reductase (AT1G77760) – were down-regulated (Moison *et al.*, 2018). None of the N-remobilization peptidases identified previously as DAPs from the proteome analyses were present in the Low-N DEGs list, except SAG12 (AT5G45890) whose transcripts were more abundant under Low-N at the opposite of its protein. Although autophagy is known to be enhanced under nitrate limitation, only the *ATG8B* (AT4G04620) gene was found over-expressed under Low-N (Avila-Ospina *et al.*, 2016). Interestingly, the *CEPD2* (AT2G47880) gene enhanced by nitrate limitation and involved downstream CEPD1 was induced, thus suggesting active shoot/root systemic N-limitation signalling under our Low-N chronic conditions (Ota *et al.*, 2020; Ruffel, 2018).

Beside these expected effects of Low-N on the N-metabolism genes, the Gene Ontology analyses showed that the major effect of Low-N on the modification of transcript pools was related to stress response and especially to plant defence and immunity (Tab.S7; Fig.9). The UP-regulated Low-N DEGs clustered many genes involved in signal transduction (receptors, activators) amongst which many *WRKY* DNA binding transcription factors (Tab.S7 and Tab.S6). Genes involved in secondary

metabolism (flavonoid synthesis, terpene degradation, abscisic acid degradation) were also up-regulated (Tab.S7).

The list of the GO terms associated to the Low-N down-regulated DEGs was quite long (Tab.S7) and reflected modifications in the response to stimuli including a large variety of stresses, as well as modification in many carbohydrate pathways. It also reflected the down-regulation of chloroplast targeted structural proteins and enzymes, that correspond to lower expression of the photosynthesis and sucrose synthesis genes. All these transcriptional modifications are consistent with the metabolic picture reflected by the proteome, and with our current knowledge of the physiological effects of nitrogen limitation on the chloroplast functions and chlorophyll contents. Due to its high nitrogen content (70% of the proteins in mesophyll cells), chloroplast represent indeed a major nitrogen source in well-feed plants (Evans & Clarke, 2019). As such, chlorophyll-meters are commonly used to detect N deficiencies during plant growth and in the field.

Nevertheless, the most surprising feature arising from the analysis of the Low-N DEGs remains the large occurrence of genes related to plant defense and immunity. It has already been reported that nitrogen shortage enhances leaf senescence, and that many leaf senescence-associated genes are related to plant response to pathogen. Here, our transcriptomic data clearly shows that growing plants under low nitrate enhances the expression of defense genes against pathogens. Whether such up-regulation of defense gene actually increased plant tolerance or resistance to pathogens, remains to be demonstrated. Several studies have suggested that plant immunity could be modulated by environmental factors as nitrogen availability (Fagard *et al.*, 2014), and several publications show that enzymes involved in nitrogen recycling may be positive factors for the plant defense against pathogens (Seifi *et al.*, 2013a; Seifi *et al.*, 2013b).

As plant density per pot was not similar under Ctrl and Low-N conditions we compared our data to the transcriptome analysis of plant competition performed by Masclaux *et al.* (2012) on Arabidopsis. Although authors found that GO terms associated to abiotic and biotic stresses were enriched in the list of the genes differentially expressed in the leaves of plant under competition, we only found 24 Up regulated genes and 66 down regulated genes in common between their study and ours. Like us Masclaux *et al.* (2012) also detected genes markers of N limitation, thus confirming response to Low-N when plants are in competition, which was the effect anticipated in our study.

Low-S transcriptomic changes reveal enhancement of autophagy gene expressions and negative impact on cell division and NIN-like protein TF family

Although the metabolome and proteome data suggested less changes under Low-S than under Low-N (Fig.3A), it was unexpected to find that the number of DEGs was considerably higher in Low-S compared to Low-N (Fig.8). Such discrepancy could be due to the fact that the proteins encoded by many of the Low-S differentially expressed genes could not be detected and quantified in our proteome.

Under Low-S, many DEGs were related to S metabolism, and also to N metabolism. The high affinity *SULTR1;1* and *SULTR1.2* sulfate transporters, the low-affinity *SULTR2;2* sulfate transporter and the *SULTR4;1* and *SULTR4;2* tonoplast efflux sulfate transporters were strongly up-regulated under Low-S. The phloem localized *SULTR1;3* and the root to shoot *SULTR3;1*, *SULTR3;4* and *SULTR3;5* transporters were at the reverse down regulated (Takahashi, 2019). Enzymes involved in S assimilation, like the ATPS1, APTS2 and ATPS4 ATP sulfurylases, were down-regulated. Only the adenosine 5'-phosphosulfate reductase APR3 was slightly enhanced. These responses to Low-S were consistent with our current knowledge from literature (Kumar *et al.*, 2017; Nath & Tuteja, 2016). Genes involved in the cysteine and methionine metabolisms were poorly modified by contrast with those involved in glucosinolate synthesis. Indeed, genes involved in glucosinolate synthesis were down-regulated under Low-S in good accordance with the changes observed at protein levels, and those involved in glucosinolate degradation were up-regulated (Tab.S6B). The DEGs related to the glutathione redox pathways were up-regulated under Low-S, which is consistent with previous reports (Smith *et al.*, 1997). Regulation of S-assimilation by transcription factors is poorly documented in plants. Our plants responded to sulfur-limitation inducing the “response to low sulfur” *LSU1* (AT3G49580), *LSU2* (AT5G24660), *LSU3* (AT3G49570) and *LSU4* (AT5G24655) genes (Sirko *et al.*, 2015; Wawrzynska & Sirko, 2014). We did not find any modification on the expression of any of the sulfur-responsive transcription factors reported so far as Prohibitin (*PHB*), Squamosa-Promoter Binding (*SPB*) and Sulfur Limitation 1 (*SLIM1*; Watanabe & Hoefgen, 2019), which was consistent with previous findings in the case of *SLIM1* (Maruyama-Nakashita *et al.*, 2006). Nevertheless, a strong induction of the *SDI1* (AT5G48850) and *SDI2* (AT1G04770) transcriptional repressors that control glucosinolate synthesis was observed (Aarabi *et al.*, 2016). The *MYB28* (AT5G61420), *MYB29* (AT5G07690) and *MYB76* (AT5G07700) involved in the regulation of the methionine-dependent glucosinolate synthesis were accordingly down-regulated, while the expression of the *MYB34* (AT5G07700), *MYB51* (AT1G18570) and *MYB122* (AT1G74080) TFs controlling the tryptophane-dependent glucosinolate pathway remained unchanged (Aarabi *et al.*, 2016).

It was actually surprising to find all the members of the NIN-LIKE PROTEIN (NLP) TF family (except NLP1 and NLP7), which are involved in the response to nitrate, down-regulated under Low-S (Chardin *et al.*, 2014; Krapp, 2015). The *bZIP1* (AT5G49450) gene that regulates nutrient responses and whose protein binds to the NLP3 promoter was by contrast induced. The *CEPR1* (AT5G49660) gene coding the shoot receptor of CEP1 root/shoot N-deficiency signal was down-regulated while the *CEPD1* (AT1G06830) gene responding to CEP1 was induced under Low-S (Ota *et al.*, 2020). The significance of such features in the response of plants to sulfur availability and in the interconnection of S and N metabolisms, remains to be elucidated. Our data indicate that Low-S modifies N-metabolism. The two *GLU1* and *GLT1* (AT5G53460) glutamate synthase genes were down-regulated under Low-S, while the *GDH2* (AT5G07440) and *GDH3* (AT3G03910) glutamate dehydrogenases were enhanced and repressed respectively. Many peptidases (*RD21A*, *RD19A*, *SAG12*) and amino acid transporters (*CAT5*, *CAT9*, *AAP2*, *LHT1* as examples; Tab.S6B) involved in N-remobilization and N-translocation, were identified in the Low-S transcriptome. The high affinity *NRT2.1* and *NRT2.6* and the low-affinity *NRT1.8* nitrate transporters are also enhanced under Low-S. Actually, the most surprising feature was about

macro-autophagy-related genes. While only one (*ATG8B*) has been found up-regulated under Low-N, the *ATG8B* (AT4G04620), *ATG8C* (AT1G62040), *ATG8D* (AT2G05630), *ATG8E* (AT2G45170), *ATG8F* (AT4G16520) and *ATG8G* (AT3G60640), *ATG12A* (AT1G54210), *ATG12B* (AT3G13970), *ATG10* (AT3G07525) and *NBR1*(AT4G24690) were enhanced under Low-S. This suggested higher autophagic activity under Low-S. The prominent role of autophagy in the response of plants to S-limitation has indeed been shown in previous reports (Zientara-Rytter *et al.*, 2011; Lornac *et al.*, 2020). Such feature is consistent with the finding that S limitation resulted in the decreases of sulfide and glucose that inhibited the TOR (Target of Rapamycin) kinase activity and enhanced autophagic activity (Dong *et al.*, 2017). In another paper, Laureano-Marin *et al* (2016) showed that sulfide inhibits the activation of autophagic activity by low nitrate in Arabidopsis roots. Finally, it was shown that sulfide controls the cytosol to nucleus movement of the GAPDH enzymes that are involved in the regulation of autophagy (Aroca *et al.*, 2017; Chang *et al.*, 2015; Henry *et al.*, 2015). Our transcriptomic results are then in line with all these reports.

The analyses of the GO terms associated to the Low-S DEGs provided deeper insights about possible physiological/cellular adaptations to the lack of sulfur (Tab.S8; Fig.9). Significant enriched terms were quite numerous for both the Low-S up-regulated and Low-S down-regulated DEGs (Tab.S8). The “Cell Component” (CC) terms associated to the up-regulated Low-S DEGs show that up-regulated DEGs were coding for proteins predicted in the vacuole, cytosol, plasma membrane, peroxisome but not in chloroplast. The enrichment of the up-regulated DEGs in genes coding ribosomal proteins was surprising regarding the lower accumulation of ribosomal proteins under Low-S as revealed by the proteomic analyses (Fig.4; Tab.S2 and Tab.S4). However, as Table S2 shows, there was almost no match between the ribosomal protein DAPs and the ribosomal protein DEGs, thus suggesting a major reprograming of the protein translation machinery under Low-S. Especially, we can see that the ribosomal proteins DAPs with lower abundance under Low-S were mainly predicted in the chloroplast and the cytosol (Tab.S2), which is in good accordance with the few down-regulated Low-S ribosomal protein genes also predicted in the chloroplast. By contrast, the up-regulated ribosomal protein genes were mainly predicted in the cytosol and the mitochondria. Enrichments in “Molecular Function” (MF) terms reflected the strong effect of Low-S on the oxidoreduction and especially on glutathione S transferase activities. The “Biological Processes” (BP), AraCyc, KEGG and Gene Family terms confirmed enrichments in genes related to response to biotic/abiotic stresses, detoxification and secondary metabolisms (phenylpropanoids, fatty acids, jasmonic acid, glutathione), which was quite consistent with the picture reflected by the Low-S proteomic data and in good agreement with previous report (Nikiforova *et al.*, 2003).

More surprising were the GO-terms associated to the Low-S down-regulated DEGs (Tab.S8). While the BP, AraCyc and Gene Family terms confirmed the down-regulation of the glucosinolate synthesis pathway and the repression of the NLP transcription factors, the CC and Gene Family terms indicated strong enrichment in genes related to cytoskeleton, phragmoplast and membrane bound organelles. Accordingly, the BP, MF and KEGG terms indicated that down-regulated DEGs were enriched in genes related to microtubule motor activity, kinesin/myosin, DNA recombination/replication/repair, nucleotide binding, telomere maintenance and, cell and chromosome organizations. Therefore, many genes

involved in the maintenance of the cell division were likely down-regulated under Low-S. Interestingly, our metabolomic data had revealed the decrease of glutathione under Low-S, and it is known that GSH movement from the cytosol to the nucleus is an important factor controlling cell cycle in mammals (Markovic *et al.*, 2007). Nuclear glutathione is necessary for safeguarding DNA integrity and the increase of the nuclear GSH pool at the onset of cell proliferation provides an appropriate redox environment for the stimulation of chromatin decompaction. The existence of movements of glutathione between cytosol and nucleus in plant cells has suggested that common redox mechanisms exist for DNA regulation in G1 and mitosis in all eukaryotes (Luis Garcia-Gimenez *et al.*, 2013; Pellny *et al.*, 2009). Although it remains to investigate whether Low-S condition affects glutathione movements from cytosol to nucleus, our data reflects here the coincidence of the perturbations of glutathione metabolism and of cell cycle.

Conclusion

Our metabolome, proteome and transcriptome study allows us to provide a comprehensive picture of how Arabidopsis adapts its physiology to nitrogen and sulfur limitations (Table 1). It first has to be noticed that there was very poor overlap between transcriptomic and proteomic changes in our study. Such feature has already been observed in other studies (Havé *et al.*, 2019; McLoughlin *et* al., 2018; Fernie and Stitt, 2012) and could be due to (i) a discrepancy in the dynamic of the protein and transcript turn overs, (ii) differences in the profundity of chemical and statistical analyses and (iii) differences in the changes related to transcription and translation/degradation processes. Nevertheless, the global picture provided by the three omics performed revealed reliable physiological changes regarding our current knowledge of how nitrogen and sulfur limitations impact metabolism (Table 1). Both Low-N and Low-S increased proteolysis, metabolite degradations, jasmonic acid signalling and secondary metabolic paths belonging to the polyphenol/flavonoid and glucosinolate pathways. Proteomic changes in glucosinolate pathway revealed different management strategies under Low-N and Low-S, with unexpected good correlation between transcript and protein changes. Low-S mostly inhibited glucosinolate synthesis while nitrogen limitation promoted glucosinolate degradation. Both strategies may save S and N sources for other metabolisms. More generally, proteomics gave a better picture of metabolic changes, while transcriptomics enlightened changes related to stress management and fundamental cellular processes.

Globally, both Low-N and Low-S resulted in (i) higher catabolic and degradation processes, (ii) increased mitochondrial metabolism and decreased chloroplast metabolic processes, (iii) lower translation and (iv) decrease of water management proteins. The main transcriptomic changes related to Low-N revealed the enhancement of plant defence and plant immunity, in line with several studies on the role of N nutrition in plant defence (Sun *et al.*, 2020; Seifi *et al.*, 2013a; Seifi *et al.*, 2013b). Transcriptomic changes under Low-S revealed the down regulation of cell division and the stimulation of autophagy. This was in good accordance with the roles of sulfide and glutathione as signals controlling cellular processes through gene regulation, or in a TOR-dependent pathway (Pellny *et al.*, 2009; Dong *et al.*, 2017; Laureano-Marin *et al.*, 2016). More striking was the inhibition under Low-S of almost all the NLP TF that are master genes of nitrate sensing (Chardin *et al.*, 2014).

While we can find in literature several omics studies that dissect the response of Arabidopsis to nitrate or sulfate starvations, it is not always easy to compare results reported due to discrepancies in growth conditions, development stages, starvation methods and duration of treatments. While we could find several reports dealing with transcriptomic and metabolomic changes, proteomic reports were more limited. In addition, many of the transcriptomic and metabolomic studies published so far, only considered changes at the root level. From the few studies performed on the rosettes of Arabidopsis plants submitted to nitrate (Scheible *et al*., 2004; *Bi et al*., 2007; Krapp *et al*., 2011) or sulfate (Hirai *et al.*, 2003; Hirai *et al.*, 2004; Nikiforova *et al*., 2003) shortages, similar effects can be extorted. Comparison of our transcriptomic results with Scheible *et al.* (2004) and Krapp *et al.* (2011) confirms the negative effect of Low-N on amino acid and tocopherol contents and the enhancement of the phenylpropanoid, sugars, starch and minor CHO pathways. Similar changes at transcriptomic levels are related to the decrease of photosynthesis (tetrapyrroles, chlorophylle, light chain, Calvin cycle) while genes involved in secondary metabolisms, TCA, mitochondria electron transport and stresses are enhanced. Krapp *et al.* (2011) also reported the positive effect of 10 days nitrate starvation on sulfate assimilation, which is also reflected by our data. The study of Bi *et al*. (2007) provides a better comparison for us, as they performed both chronic and short term starvations on Arabidopsis adult plants under short days. The main results they found as (i) the decrease of *NR* and *NiR* transcripts and increase of *GLN1;1* and *GLN1;4* ones, (ii) the enhancement of genes related to biotic and abiotic stresses, (iii) the increase of secondary metabolism, anthocyanin and phenylpropanoid gene expression and (iv) the enhancement of bioprocesses related to N assimilation, nutrient transport, cell homeostasis and S assimilation, are globally consistent with our finding. It is also noticeable that the signature of Low-N effects on metabolome and transcriptome have many similarities with the signatures reported by Watanabe *et al.* (2013) and Guo *et al.* (2004) for leaf senescence.

The recent review of Watanabe and Hoefgen (2019) facilitated our exploration of the correspondence between our results and former studies dealing with S starvation. Although Nikiforova *et al.* (2003) performed S starvation using seedlings grown in vitro in plates, many of their findings are reliable with our study. Like us they found exacerbation of sulfur assimilation and especially transporters and of flavonoid and jasmonic acid pathways. They reported effects on cell rescue and defence, cell death and ageing, energy metabolism, protein synthesis and transport facilitation. In addition, they observed like us the positive effect of S starvation on the degradation of S compounds and especially on glucosinolate catabolism. In their review, Hirai and Saito (2004) summarized the effects of short term and long term S deficiency found by Hirai *et al.* (2003, 2004), Nikiforova *et al*. (2003) and Maruyama-Nakashita *et al.* (2003) on the jasmonic acid, oxidative stress and flavonoid pathways. Interestingly, D'Hooghe *et al.* (2013) reported similar effects on the proteome on *Brassica napus.* The meta-analysis recently performed by Henriquez-Valencia et al. (2018) on root transcriptomes brings also some intelligible correspondences with our findings like effects of S starvation on carbohydrates metabolism, nitrogen transport and proteolysis.

In addition of the several correspondences found between our study and literature, especially regarding the effects Low-S, our study describes for the first time the effect of Low-S on cell division, autophagy and NLP gene expressions.

Acknowledgement:

Authors thank Fabienne Soulay, Joël Talbotec and Philippe Maréchal (IJPB, INRA Versailles) for taking care of plants, Fabien Chardon (IJPB, INRA Versailles) for discussion and advices.

Financial supports:

This work was supported the ANR-12-ADAPT-0010-0. The LabEx Saclay Plant Sciences-SPS (ANR-10-LABX-0040-SPS) provided support for IJPB and the POPS platform in charge of RNA-seq (IPS2 Orsay France). J.L. was supported by Agreenskills international program for mobility with the support of the AgreenSkills+ fellowship program which has received funding from the EU's Seventh Framework Program under agreement N° FRP7-609398 (AgreenSkill+ contract). M.H. was supported by ANR-12-ADAPT-0010-0. Funds for RNAseq were provided to J.L. by the National Natural Science Foundation of China (NSFC accession No. 31901282).

Contribution of authors:

M.H. and T.B. performed proteomic experiments under the supervision of M.Z. Lipid analyses were performed by F.T.. Metabalomic GC-MS analyses were performed by G.C.. Cofactor LC-MS analyses were performed by F.G.. RNA-seq was performed on the POPS platform by A.L-A.. J.L. performed statistical and bioinformatic analyses. C.M-D. and J.L. contributed to the data mining and wrote the paper. Both C.M-D. and J.L. obtained financial support for the study. C.M-D. supervised the entire work.

Table 1: Summary of the major changes on metabolome, proteome and transcriptome observed in Arabidopsis rosettes under Low-N and Low-S. CHO, carbohydrates; TCA, Tricarboxylic acid cycle; GSH, reduced glutathione; Glu, glutamate; Asp, aspartate; Met, methionin; Trp, tryptophane; Gln, glutamine; Pro, proline; Orn, ornithine; Ser, serine; Gly, glycine; Thr, threonine; Ala, alanine, OPP, pentose phosphate pathway.

Metabolome	Proteome	Transcriptome
Low-N		
Carbohydrates (Lipids, CHO, TCA) ↑	Cell wall degradation ↑	Defence, immunity ↑
ATP ↓ ADP ↑	Lipid and starch degradation ↑	WRKY TF ↑
Dehydroascorbate α-Tocopherol ↑	Amino acid degradation ↑	Flavonoid pathways ↑
GSH ↓ GSSG ↑	Protein degradation ↑	ABA and Terpenoide degradations ↑
Glu, Asp, Met, Trp ↑	Antioxidants ↑	Chloroplast lipid metabolism ↓
Gln, Pro, Orn ↓	Jasmonate synthesis ↑	Chloroplast fatty acid synthesis ↓
Ser, Gly, Thr, Ala ↓	TCA, OPP ↑	Amine metabolism ↓
Spermidine, putrescine ↓	Ribosomes ↓	Glucosinolate metabolism ↓
	Photosynthesis, photorespiration ↓	Sucrose synthesis ↓
	Fatty acid synthesis ↓	Water channels ↓
	Aquaporins ↓	
	Whirly1 ↓	
Low-S		
Lipids ↓	Lipid and starch degradation ↑	Flavonoid pathways ↑
Glu, Fru, Myo-inositol ↓	Amino acid degradation ↑	Cytoplasmic ribosomes ↑
Glu-6P, Fru-6P, Myo-inositol1P ↑	Protein degradation ↑	N remobilization, autophagy, proteolysis ↑
GSH ↓ GSSG ↓	Jasmonate synthesis ↑	Jasmonate synthesis ↑
Leu, Asp, Ser, Gly, Thr, Ala ↑	TCA ↑	N assimilation ↓
Orn ↓	Ribosomes ↓	S assimilation ↓
	Photosynthesis, photorespiration ↓	Glucosinolate synthesis ↓
	Fatty acid synthesis ↓	Chloroplast metabolism ↓
	Aquaporin ↓	Translation ↓
	Whirly1 ↓	Cell division ↓
	Glutathione S-transferase ↓	Cytoskeleton, DNA replication, repair ↓
	Glucosinolate synthesis ↓	NLP NIN-like TF ↓
	Energy metabolism ↓	

Legend of Figures

Figure 1: Metabolite changes under low nitrate (Low-N) condition relative to the control (Ctrl) growth condition. The relative metabolite concentrations were measured on the rosettes of plants grown under low nitrate or control conditions for 60 days. Note that when the calculated fold changes (FC) in the Low-N relative to Ctrl condition indicated a decrease (i.e. 0<FC<1), the values were changed to [-1/(calculated FC)] in the figure. Then the FC values ranged between -4 and 4 according to the colour code from blue to red. FC are only shown for metabolites significantly different between low N and Ctrl conditions (t-test p-value ≤ 0.05). Negative number means metabolite less abundant in said condition and positive number means metabolite more abundant in said condition. All the metabolites were quantified using GC-MS except those indicated by * that were quantified using LC-MS.

Figure 2. Metabolite changes under low sulfate (Low-S) conditions relative to the control (Ctrl) growth condition. The relative metabolite concentrations were measured on the rosettes of plants grown under low sulfate or control conditions for 60 days. Note that when the calculated fold changes (FC) in the Low-S relative to Ctrl conditions indicated a decrease (i.e. 0<FC<1), the values were changed to [-1/(calculated FC)] in the figure. Then the FC values ranged between -4 and 4 according to the colour code from blue to red. Negative number means metabolite less abundant in said condition and positive number means metabolite more abundant in said condition. The same metabolites as in Figure 1 are presented. FC are only shown for metabolites significantly different between low S and Ctrl conditions (t-test p-value ≤ 0.05). All the metabolites were quantified using GC-MS except those indicated by * that were quantified using LC-MS.

Figure 3: Proteins significantly differentially accumulated (DAPs) under Low-N or Low-S relative to Ctrl. The numbers of up-accumulated (UP) and depleted (DOWN) DAPs under Low-N and Low-S are presented (A). Cellular predicted localisation of DAPs under Low-N or Low-S conditions according to SUBA 4 (B). Significant enrichments of Gene Ontology, Gene Family, AraCyc pathway and KEGG terms for the DAPs accumulated (Red) or less abundant (Blue) under Low-N or Low-S. Significant terms were identified using the VirtualPlant 1.3 BioMaps tool (http://virtualplant.bio.nyu.edu/cgi-bin/vpweb/) applying a P-value cut off of 0.05.

Figure 4: Proteomic changes in amino acid pathway under low nitrate and low sulfate conditions. Significant differentially accumulated proteins (DAPs; big squares; t-test P-value ≤ 0.05) and differentially accumulated metabolites (grey-surrounded small squares) belonging to amino acid metabolism. Fold changes under Low-N (left) and Low-S (right) conditions are shown. Note that like for metabolites in Fig.1 and 2, when the calculated fold changes (FC) in the Low S or Low-N conditions relative to Ctrl conditions indicated a decrease (i.e. 0<FC<1), the values were changed to [-1/(calculated FC)] in the figure. The colour codes from blue to red represent fold change values ranging between -4

and 4. Negative number means protein less abundant in said condition and positive number means protein more abundant in said condition. White squares indicate non significant changes. Series of four numbers in the figure indicate E.C. enzyme numbers. ASP: aspartate aminotransferase; GDH: glutamate dehydrogenase; GOGAT: glutamate synthase; GS: glutamine synthetase; P5CS1: delta1-pyrroline-5-carboxylate synthetase; GSH: reduced glutathione form; GSSG: oxidized glutathione; SiR: sulfite reductase; ATPS: ATP sulfurylase; CGS1: cystathionine gamma-synthase; MS2: methionine synthase.

Figure 5: Low nitrate and low sulfate conditions affect protein synthesis and protein degradation in opposite ways. Significant differentially accumulated proteins (DAPs; t-test P-value ≤ 0.05) involved in protein degradation (A) and protein synthesis (B) and translation (C) under Low-N (left) and Low-S (right) conditions. Note that when the calculated fold changes (FC) in the Low-N relative to Ctrl condition indicated a decrease (i.e. 0<FC<1), the values were changed to [-1/(calculated FC)] in the figure. Then the FC values ranged between -4 and 4 according to the colour code from blue to red. FC are only shown for proteins significantly different between Low-N or Low-S and Ctrl conditions. Negative number means protein less abundant in said condition and positive number means protein more abundant in said condition. White square indicate non significant changes.

Figure 6: Changes in proteins involved in photosynthesis and photorespiration under low nitrate and low sulfate conditions. Significant differentially accumulated proteins (DAPs; t-test P-value ≤ 0.05) involved in chloroplast carbon fixation and photorespiration under Low-N (left) and Low-S (right) conditions. Note that when the calculated fold changes (FC) in the Low-N relative to Ctrl condition indicated a decrease (i.e. 0<FC<1), the values were changed to [-1/(calculated FC)] in the figure. Then the FC values ranged between -4 and 4 according to the colour code from blue to red. FC are only shown for proteins significantly different between Low-N or Low-S and Ctrl conditions. Negative number means protein less abundant in said condition and positive number means protein more abundant in said condition. Series of four numbers in the figure indicate E.C. enzyme numbers. White squares indicate non significant changes.

Figure 7: Abundance of proteins involved in glycolysis, TCA cycle and pentose phosphate pathway increased under Low-N and Low-S conditions. Significant differentially accumulated proteins (DAPs; t-test P-value ≤ 0.05) under Low-N (left) and Low-S (right) conditions are shown. Note that when the calculated fold changes (FC) in the Low-N relative to Ctrl condition indicated a decrease (i.e. 0<FC<1), the values were changed to [-1/(calculated FC)] in the figure. Then the FC values ranged between -4 and 4 according to the colour code from blue to red. FC are only shown for proteins significantly different between Low-N or Low-S and Ctrl conditions. Negative number means protein less abundant in said condition and positive number means protein more abundant in said condition. Series

of four numbers in the figure indicate E.C. enzyme numbers. White squares indicate non significant changes.

Figure 8: Both low sulfate and low nitrate modify protein content of enzymes involved in sufate assimilation, glutathione and glucosinolate metabolisms. Significant differentially accumulated proteins (DAPs; t-test P-value ≤ 0.05) involved in sufate assimilation (A) glutathione (B) and glucosinolate (C) metabolisms under Low-N (left) and Low-S (right) conditions. Note that when the calculated fold changes (FC) in the Low-N relative to Ctrl condition indicated a decrease (i.e. 0<FC<1), the values were changed to [-1/(calculated FC)] in the figure. Then the FC values ranged between -4 and 4 according to the colour code from blue to red. FC are only shown for proteins significantly different between Low-N or Low-S and Ctrl conditions. Negative number means protein less abundant in said condition and positive number means protein more abundant in said condition. Series of four numbers in the figure indicate E.C. enzyme numbers. White squares indicate non significant changes.

Figure 9: Transcriptomic changes reveal specific effects of Low-N and Low-S conditions. Venn diagram (at the top) presents the number of differentially expressed genes (DEGs) under Low-N, Low-S and in intersection both Low-N and Low-S conditions. The number of up-regulated genes under Low-N or Low-S is indicated above and the number of down-regulated genes below. Significant enrichments in Gene Ontology, Gene Family, AraCyc pathway and KEGG terms for the up-regulated (Red) or dow-regulated (Blue) DEGs under Low-N (left) or Low-S (right) are shown. Significant terms were identified using the VirtualPlant 1.3 BioMaps tool (http://virtualplant.bio.nyu.edu/cgi-bin/vpweb/) applying a *P*-value cut off of at least 0.01 (see Tab.S7 and S8).

Supplementary material:

Figure S1: Phenotype of Col-0 plants grown under Control (Ctrl; bottom), Low-N (up left) and Low-S (top right) conditions for 60 days after sowing.

Figure S2: Venn analyses of the differentially expressed genes (DEGs) under Low-N and Low-S conditions.

Table S1: Nutritive Stock solutions for plant growth on sand.

Table S2A,B,C: lists of the significant differentially accumulated proteins (DAPs) under low N (A) and low S (B) conditions. C combines chances in Low-N and Low-S.

Table S3: List of the AraCyc pathways, KEGG pathway and GENE Family terms significantly enriched in the list of the differentially accumulated proteins (DAPs).

Table S4: List of the AraCyc pathways, KEGG pathway and GENE Family terms significantly enriched in the list of the differentially accumulated proteins (DAPs).

Table S5: lists of the common significant differentially accumulated proteins (DAPs) under both Low-N and Low-S conditions.

Table S6A,B,C: Significant differentially expressed genes (DEGs) identified under low N (A) and low S (B) conditions, and common to low-N and low-S (C).

Table S7: Analysis of GO, Aracyc, KEGG, Gene Family terms on the Low-N DEG lists.

Table S8: Analysis of GO, Aracyc, KEGG, Gene Family terms on the Low-S DEG lists.

References

Aarabi F, Kusajima M, Tohge T, Konishi T, Gigolashvili T, Takamune M, Sasazaki Y, Watanabe M, Nakashita H, Fernie AR, Saito K, Takahashi H, Hubberten HM, Hoefgen R, Maruyama-Nakashita A. 2016. Sulfur deficiency-induced repressor proteins optimize glucosinolate biosynthesis in plants. Science Advances **2**.

Aroca A, Schneider M, Scheibe R, Gotor C, Romero LC. 2017. Hydrogen Sulfide Regulates the Cytosolic/Nuclear Partitioning of Glyceraldehyde-3-Phosphate Dehydrogenase by Enhancing its Nuclear Localization. Plant and Cell Physiology **58**, 983-992.

Avila-Ospina L, Clément G, Masclaux-Daubresse C. 2017. Metabolite profiling for leaf senescence in barley reveals decreases in amino acids and glycolysis intermediates. Agronomy-Basel **7(1) 15**

Avila-Ospina L, Marmagne A, Soulay F, Masclaux-Daubresse C. 2016. Identification of Barley (Hordeum vulgare L.) Autophagy Genes and Their Expression Levels during Leaf Senescence, Chronic Nitrogen Limitation and in Response to Dark Exposure. Agronomy-Basel **6**.

Balliau T, Blein-Nicolas M, Zivy M. 2018. Evaluation of Optimized Tube-Gel Methods of Sample Preparation for Large-Scale Plant Proteomics. Proteomes **6**, 6.

Barney PE, Bush LP. 1985. Interaction of nitrate and sulfate reduction in tobacco .1. Influence of availability of nitrate and sulfate. Journal of Plant Nutrition **8**, 505-515.

Bi YM, Wang RL, Zhu T, Rothstein SJ. 2007. Global transcription profiling reveals differential responses to chronic nitrogen stress and putative nitrogen regulatory components in Arabidopsis. BMC Genomics **8**.

Bolger A, Lohse M, Usadel B. 2014. Trimmomatic: a flexible trimmer for Illumina sequence data. Bioinformatics **30**, 2114-2120.

Bonnot T, Martre P, Hatte V, Dardevet M, Leroy L, Bénard C, Falagán N, Martin-Magniette M-L, Deborde C, Moing A, Gibon Y, Pailloux M, Bancel E, Ravel C. 2020. Omics data reveal putative regulators of einkorn grain protein composition under sulfur deficiency. Plant Physiology **183**, 501-516.

Cataldo DA, Haroon M, Schrader LE, Young VL. 1975. Rapid colorimetric determination of nitrate in plant tissue by nitration of salicylic acid. Commun. Soil Science and plant analysis **6**, 71-80.

Chan KX, Phua SY, Van Breusegem F. 2019. Secondary sulfur metabolism in cellular signalling and oxidative stress responses. Journal of Experimental Botany **70**, 4237-4250.

Chang CM, Su H, Zhang DH, Wang YS, Shen QH, Liu B, Huang R, Zhou TH, Peng C, Wong CCL, Shen HM, Lippincott-Schwartz J, Liu W. 2015. AMPK-Dependent Phosphorylation of GAPDH Triggers Sirt1 Activation and Is Necessary for Autophagy upon Glucose Starvation. Molecular Cell **60**, 930-940.

Chardin C, Girin T, Roudier F, Meyer C, Krapp A. 2014. The plant RWP-RK transcription factors: key regulators of nitrogen responses and of gametophyte development. Journal of Experimental Botany **65**, 5577-5587.

Clément G, Moison M, Soulay F, Reisdorf-Cren M, Masclaux-Daubresse C. 2018. Metabolomics of laminae and midvein during leaf senescence and source-sink metabolite management in Brassica napus L. leaves. Journal of Experimental Botany **69**, 891-903.

Comadira G, Rasool B, Kaprinska B, Garcia BM, Morris J, Verrall SR, Bayer M, Hedley PE, Hancock RD, Foyer CH. 2015. WHIRLY1 Functions in the Control of Responses to Nitrogen Deficiency But Not Aphid Infestation in Barley. Plant Physiology **168**, 1140-+.

Courbet G, Gallardo K, Vigani G, Brunel-Muguet S, Trouverie J, Salon C, Ourry A. 2019. Disentangling the complexity and diversity of crosstalk between sulfur and other mineral nutrients in cultivated plants. Journal of Experimental Botany **70**, 4183-4196.

Dai ZW, Plessis A, Vincent J, Duchateau N, Besson A, Dardevet M, Prodhomme D, Gibon Y, Hilbert G, Pailloux M, Ravel C, Martre P. 2015. Transcriptional and metabolic alternations rebalance wheat grain storage protein accumulation under variable nitrogen and sulfur supply. Plant Journal **83**, 326-343.

De Angeli A, Monachello D, Ephritikhine G, Frachisse JM, Thomine S, Gambale F, Barbier-Brygoo H. 2006. The nitrate/proton antiporter AtCLCa mediates nitrate accumulation in plant vacuoles. Nature **442**, 939-942.

Desclos M, Etienne P, Coquet L, Jouenne T, Bonnefoy J, Segura R, Reze S, Ourry A, Avice JC. 2009. A combined 15N tracing/proteomics study in *Brassica napus* reveals the chronology of proteomics events associated with N remobilisation during leaf senescence induced by nitrate limitation or starvation. Proteomics **9**, 3580-3608.

D'Hooghe P, Escamez S, Trouverie J, Avice JC. 2013. Sulphur limitation provokes physiological and leaf proteome changes in oilseed rape that lead to perturbation of sulphur, carbon and oxidative metabolisms. BMC Plant Biology **13**.

D'Hooghe P, Dubousset L, Gallardo K, Kopriva S, Avice JC, Trouverie J. 2014. Evidence for Proteomic and Metabolic Adaptations Associated with Alterations of Seed Yield and Quality in Sulfur- limited Brassica napus L. Molecular & Cellular Proteomics **13**, 1165-1183.

Diaz C, Lemaitre T, Christ A, Azzopardi M, Kato Y, Sato F, Morot-Gaudry JF, Le Dily F, Masclaux-Daubresse C. 2008. Nitrogen recycling and remobilization are differentially controlled by leaf senescence and development stage in Arabidopsis under low nitrogen nutrition. Plant Physiology **147**, 1437-1449.

Dong YH, Silbermann M, Speiser A, Forieri I, Linster E, Poschet G, Samami AA, Wanatabe M, Sticht C, Teleman AA, Deragon JM, Saito K, Hell R, Wirtz M. 2017. Sulfur availability regulates plant growth via glucose-TOR signaling. Nature Communications **8**.

Engelsberger WR, Schulze WX. 2012. Nitrate and ammonium lead to distinct global dynamic phosphorylation patterns when resupplied to nitrogen-starved Arabidopsis seedlings. Plant Journal **69**, 978-995.

Evans JR, Clarke VC. 2019. The nitrogen cost of photosynthesis. Journal of Experimental Botany **70**, 7-15.

Fagard M, Launay A, Clément G, Courtial J, Dellagi A, Farjad M, Krapp A, Soulié M-C, Masclaux-Daubresse C. 2014. Nitrogen metabolism meets phytopathology. J Exp Bot **65**, 5643-5656.

Fernie AR, Stitt M. 2012. On the Discordance of Metabolomics with Proteomics and Transcriptomics: Coping with Increasing Complexity in Logic, Chemistry, and Network Interactions. Plant Physiology **158**, 1139-1145.

Garai S, Tripathy BC. 2018. Alleviation of Nitrogen and Sulfur Deficiency and Enhancement of Photosynthesis in Arabidopsis thaliana by Overexpression of Uroporphyrinogen III Methyltransferase (UPM1) (vol 8, pg 2265, 2018). Frontiers in Plant Science **9**.

Gironde A, Dubousset L, Trouverie J, Etienne P, Avice JC. 2014. The impact of sulfate restriction on seed yield and quality of winter oilseed rape depends on the ability to remobilize sulfate from vegetative tissues to reproductive organs. Frontiers in plant science **5**.

Guerard F, Petriacq P, Gakiere B, Tcherkez G. 2011. Liquid chromatography/time-of-flight mass spectrometry for the analysis of plant samples: A method for simultaneous screening of common cofactors or nucleotides and application to an engineered plant line. Plant Physiology and Biochemistry **49**, 1117-1125.

Guo Y, Cai Z, Gan S. 2004. Transcriptome of Arabidopsis leaf senescence. Plant and Cell Environement **27**, 521-549.

Hacham Y, Matityahu I, Amir R. 2013. Light and sucrose up-regulate the expression level of Arabidopsis cystathionine gamma-synthase, the key enzyme of methionine biosynthesis pathway. Amino acids **45**, 1179-1190.

Havé M, Balliau T, Cottyn-Boitte B, Derond E, Cueff G, Soulay F, Lornac A, Reichman P, Dissmeyer N, Avice J-C, Gallois P, Rajjou L, Zivy M, Masclaux-Daubresse C. 2018. Increase of proteasome and papain-like cysteine protease activities in autophagy mutants: backup compensatory effect or pro cell-death effect? Journal of Experimental Botany **69**, 1369-1385.

Havé M, Luo J, Tellier F, Balliau T, Cueff G, Chardon F, Zivy M, Rajjou L, Cacas J-L, Masclaux-Daubresse C. 2019. Proteomic and lipidomic analyses of the Arabidopsis atg5 autophagy mutant reveal major changes in ER and peroxisome metabolisms and in lipid composition New Phytologist **223**, 1461-1477.

Havé M, Marmagne A, Chardon F, Masclaux-Daubresse C. 2017. Nitrogen remobilization during leaf senescence: lessons from Arabidopsis to crops. Journal of Experimental Botany **68**, 2513-2529.

Henriquez-Valencia C, Arenas A, Medina J, Canales J. 2018. Integrative Transcriptomic Analysis Uncovers Novel Gene Modules That Underlie the Sulfate Response in Arabidopsis thaliana. Frontiers in Plant Science **9**.

Henry E, Fung N, Liu J, Drakakaki G, Coaker G. 2015. Beyond Glycolysis: GAPDHs Are Multi-functional Enzymes Involved in Regulation of ROS, Autophagy, and Plant Immune Responses. PLoS genetics **11**.

Higashi Y, Hirai MY, Fujiwara T, Naito S, Noji M, Saito K. 2006. Proteomic and transcriptomic analysis of Arabidopsis seeds: molecular evidence for successive processing of seed proteins and its implication in the stress response to sulfur nutrition. Plant Journal **48**, 557-571.

Hirai M, Fujikawa Y, Yano M, Dayan G, Kanaya S, Saito K. 2004. Transcriptome and metabolome analyses reveal a whole adaptive process of plant to sulfur deficiency. Plant and Cell Physiology **45**, S122-S122.

Hirai MY, Fujiwara T, Awazuhara M, Kimura T, Noji M, Saito K. 2003. Global expression profiling of sulfur-starved Arabidopsis by DNA macroarray reveals the role of O-acetyl-L-serine as a general regulator of gene expression in response to sulfur nutrition. Plant Journal **33**, 651-663.

Hirai MY, Saito K. 2004. Post-genomics approaches for the elucidation of plant adaptive mechanisms to sulphur deficiency. Journal of Experimental Botany **55**, 1871-1879.

James M, Poret M, Masclaux-Daubresse C, Marmagne A, Coquet L, Jouenne T, Chan P, Trouverie J, Etienne P. 2018. SAG12, a Major Cysteine Protease Involved in Nitrogen Allocation during Senescence for Seed Production in Arabidopsis thaliana. Plant and Cell Physiology **59**, 2052-2063.

Jobe TO, Zenzen I, Karvansara PR, Kopriva S. 2019. Integration of sulfate assimilation with carbon and nitrogen metabolism in transition from C-3 to C-4 photosynthesis. Journal of Experimental Botany **70**, 4211-4221.

Kopriva S. 2006. Regulation of sulfate assimilation in Arabidopsis and beyond. Annals of Botany **97**, 479-495.

Kopriva S, Rennenberg H. 2004. Control of sulphate assimilation and glutathione synthesis: interaction with N and C metabolism. Journal of Experimental Botany **55**, 1831-1842.

Kopylova E, Noé L, Touzet H. 2012. SortMeRNA:fast and accurate filtering of ribosomal RNAs in metatranscritomic data. Bioinformatics **28**, 3211-3217.

Krapp A. 2015. Plant nitrogen assimilation and its regulation: a complex puzzle with missing pieces. Current Opinion in Plant Biology **25**, 115-122.

Krapp A, Berthome R, Orsel M, Mercey-Boutet S, Yu A, Castaings L, Elftieh S, Major H, Renou J-P, Daniel-Vedele F. 2011. Arabidopsis Roots and Shoots Show Distinct Temporal Adaptation Patterns toward Nitrogen Starvation. Plant Physiology **157**, 1255-1282.

Krupinska K, Braun S, Nia MS, Schafer A, Hensel G, Bilger W. 2019. The nucleoid-associated protein WHIRLY1 is required for the coordinate assembly of plastid and nucleus-encoded proteins during chloroplast development. Planta **249**, 1337-1347.

Kumar S, Verma S, Trivedi PK. 2017. Involvement of Small RNAs in Phosphorus and Sulfur Sensing, Signaling and Stress: Current Update. Frontiers in Plant Science **8**.

Laureano-Marin AM, Moreno I, Romero LC, Gotor C. 2016. Negative Regulation of Autophagy by Sulfide Is Independent of Reactive Oxygen Species. Plant Physiology **171**, 1378-1391.

Lee S, Kang BS. 2005. Interaction of sulfate assimilation with nitrate assimilation as a function of nutrient status and enzymatic co-regulation in Brassica juncea roots. Journal of Plant Biology **48**, 270-275.

Lezhneva L, Kiba T, Feria-Bourrellier A-B, Lafouge F, Boutet-Mercey S, Zoufan P, Sakakibara H, Daniel-Vedele F, Krapp A. 2014. The Arabidopsis nitrate transporter NRT2.5 plays a role in nitrate acquisition and remobilization in nitrogen-starved plants. Plant Journal **80**, 230-241.

Liao Y, Smyth GK, Shi W. 2013. The Subread aligner: fast, accurate and scalable read mapping by seed-and-vote. Nucleic Acids Research **41**.

Liao Y, Smyth GK, Shi W. 2014. featureCounts: an efficient general purpose program for assigning sequence reads to genomic features. Bioinformatics **30**, 923-930.

Lin WF, Huang DM, Shi XM, Deng B, Ren YJ, Lin WX, Miao Y. 2019. H2O2 as a Feedback Signal on Dual-Located WHIRLY1 Associates with Leaf Senescence in Arabidopsis. Cells **8**.

Lornac A, Have M, Chardon F, Soulay F, Clement G, Avice J-C, Masclaux-Daubresse C. 2020. Autophagy Controls Sulphur Metabolism in the Rosette Leaves of Arabidopsis and Facilitates S Remobilization to the Seeds. Cells **9**.

Lothier J, Gaufichon L, Sormani R, Lemaitre T, Azzopardi M, Morin H, Chardon F, Reisdorf-Cren M, Avice J-C, Masclaux-Daubresse C. 2011. The cytosolic glutamine synthetase GLN1;2 plays a role in the control of plant growth and ammonium homeostasis in Arabidopsis rosettes when nitrate supply is not limiting. Journal of Experimental Botany **62**, 1375-1390.

Loudet O, Chaillou S, Merigout P, Talbotec J, Daniel-Vedele F. 2003. Quantitative trait loci analysis of nitrogen use efficiency in Arabidopsis. Plant Physiol **131**, 345-358.

Love MI, Huber W, Anders S. 2014. Moderated estimation of fold change and dispersion for RNA-seq data with DESeq2. Genome Biology **15**.

Luis Garcia-Gimenez J, Markovic J, Dasi F, Queval G, Schnaubelt D, Foyer CH, Pallardo FV. 2013. Nuclear glutathione. Biochimica Et Biophysica Acta-General Subjects **1830**, 3304-3316.

Lyutvinskiy Y, Yang HQ, Rutishauser D, Zubarev RA. 2013. In Silico Instrumental Response Correction Improves Precision of Label-free Proteomics and Accuracy of Proteomics-based Predictive Models. Molecular & Cellular Proteomics **12**, 2324-2331.

Markovic J, Borras C, Ortega A, Sastre J, Vina J, Pallardo FV. 2007. Glutathione is recruited into the nucleus in early phases of cell proliferation. Journal of Biological Chemistry **282**, 20416-20424.

Maruyama-Nakashita A, Inoue E, Watanabe-Takahashi A, Yarnaya T, Takahashi H. 2003. Transcriptome profiling of sulfur-responsive genes in Arabidopsis reveals global effects of sulfur nutrition on multiple metabolic pathways. Plant Physiology **132**, 597-605.

Maruyama-Nakashita A, Nakamura Y, Tohge T, Saito K, Takahashi H. 2006. Arabidopsis SLIM1 is a central transcriptional regulator of plant sulfur response and metabolism. Plant Cell **18**, 3235-3251.

Marshall RS, Li FQ, Gemperline DC, Book AJ, Vierstra RD. 2015. Autophagic degradation of the 26S proteasome Is mediated by the dual ATG8/Ubiquitin receptor RPN10 in Arabidopsis. Molecular Cell **58**, 1053-1066.

Masclaux-Daubresse C, Daniel-Vedele F, Dechorgnat J, Chardon F, Gaufichon L, Suzuki A. 2010. Nitrogen uptake, assimilation and remobilization in plants: challenges for sustainable and productive agriculture. Annals of Botany **105**, 1141-1157.

Masclaux FG, Bruessow F, Schweizer F, Gouhier-Darimont C, Keller L, Reymond P. 2012. Transcriptome analysis of intraspecific competition in Arabidopsis thaliana reveals organ-

specific signatures related to nutrient acquisition and general stress response pathways. Bmc Plant Biology **12**.

McLoughlin F, Augustine RC, Marshall RS, Li FQ, Kirkpatrick LD, Otegui MS, Vierstra RD. 2018. Maize multi-omics reveal roles for autophagic recycling in proteome remodelling and lipid turnover. Nature Plants **4**, 1056-1070.

McNeill AM, Eriksen J, Bergstrom L, Smith KA, Marstorp H, Kirchmann H, Nilsson I. 2005. Nitrogen and sulphur management: challenges for organic sources in temperate agricultural systems. Soil Use and Management **21**, 82-93.

Medici A, Szponarski W, Dangeville P, Safi A, Dissanayake IM, Saenchai C, Emanuel A, Rubio V, Lacombe B, Ruffel S, Tanurdzic M, Rouached H, Krouk G. 2019. Identification of Molecular Integrators Shows that Nitrogen Actively Controls the Phosphate Starvation Response in Plants. Plant Cell **31**, 1171-1184.

Meyer C, Lea US, Provan F, Kaiser WM, Lillo C. 2005. Is nitrate reductase a major player in the plant NO (nitric oxide) game? Photosynthesis Research **83**, 181-189.

Moison M, Marmagne A, Dinant S, Soulay F, Azzopardi M, Lothier J, Citerne S, Morin H, Legay N, Chardon F, Avice JC, Reisdorf-Cren M, Masclaux-Daubresse C. 2018. Three cytosolic glutamine synthetase isoforms localized in different-order veins act together for N remobilization and seed filling in Arabidopsis. Journal of Experimental Botany **69**, 4379-4393.

Nath M, Tuteja N. 2016. NPKS uptake, sensing, and signaling and miRNAs in plant nutrient stress. Protoplasma **253**, 767-786.

Nikiforova V, Freitag J, Kempa S, Adamik M, Hesse H, Hoefgen R. 2003. Transcriptome analysis of sulfur depletion in Arabidopsis thaliana: interlacing of biosynthetic pathways provides response specificity. Plant Journal **33**, 633-650.

Ota R, Ohkubo Y, Yamashita Y, Ogawa-Ohnishi M, Matsubayashi Y. 2020. Shoot-to-root mobile CEPD-like 2 integrates shoot nitrogen status to systemically regulate nitrate uptake in Arabidopsis. Nature communications **11**.

Pellny TK, Locato V, Vivancos PD, Markovic J, De Gara L, Pallardo FV, Foyer CH. 2009. Pyridine Nucleotide Cycling and Control of Intracellular Redox State in Relation to Poly (ADP-Ribose) Polymerase Activity and Nuclear Localization of Glutathione during Exponential Growth of Arabidopsis Cells in Culture. Molecular Plant **2**, 442-456.

Postles J, Curtis TY, Powers SJ, Elmore JS, Mottram DS, Halford NG. 2016. Changes in Free Amino Acid Concentration in Rye Grain in Response to Nitrogen and Sulfur Availability, and Expression Analysis of Genes Involved in Asparagine Metabolism. Frontiers in Plant Science **7**.

Pružinská A, Shindo T, Niessen S, Kaschani F, Tóth R, Millar AH, van der Hoorn RAL. 2017. Major Cys protease activities are not essential for senescence in individually darkened Arabidopsis leaves. BMC Plant Biology **17**, DOI: 10.1186/s12870-12016-10955-12875.

Ren YJ, Li YY, Jiang YQ, Wu BH, Miao Y. 2017. Phosphorylation of WHIRLY1 by CIPK14 Shifts Its Localization and Dual Functions in Arabidopsis. Molecular Plant **10**, 749-763.

Ristova D, Carre C, Pervent M, Medici A, Kim GJ, Scalia D, Ruffel S, Birnbaum KD, Lacombe B, Busch W, Coruzzi GM, Krouk G. 2016. Combinatorial interaction network of transcriptomic

and phenotypic responses to nitrogen and hormones in the Arabidopsis thaliana root. Science Signaling **9**.

Robertson GP, Vitousek PM. 2009. Nitrogen in Agriculture: Balancing the Cost of an Essential Resource. Annual Review of Environment and Resources **34**, 97-125.

Ruffel S. 2018. Nutrient-Related Long-Distance Signals: Common Players and Possible Cross-Talk. Plant and Cell Physiology **59**, 1723-1732.

Scheible WR, Morcuende R, Czechowski T, Fritz C, Osuna D, Palacios-Rojas N, Schindelasch D, Thimm O, Udvardi MK, Stitt M. 2004. Genome-wide reprogramming of primary and secondary metabolism, protein synthesis, cellular growth processes, and the regulatory infrastructure of Arabidopsis in response to nitrogen. Plant Physiol **136**, 2483-2499.

Seifi HS, Curvers K, De Vleesschauwer D, Delaere I, Aziz A, Hofte M. 2013a. Concurrent overactivation of the cytosolic glutamine synthetase and the GABA shunt in the ABA-deficient sitiens mutant of tomato leads to resistance against Botrytis cinerea. New Phytologist **199**, 490-504.

Seifi HS, Van Bockhaven J, Angenon G, Hofte M. 2013b. Glutamate Metabolism in Plant Disease and Defense: Friend or Foe? Molecular Plant-Microbe Interactions **26**, 475-485.

Sirko A, Wawrzynska A, Rodriguez MC, Sektas P. 2015. The family of LSU-like proteins. Frontiers in Plant Science **5**.

Smith FW, Hawkesford MJ, Ealing PM, Clarkson DT, VandenBerg PJ, Belcher AR, Warrilow GS. 1997. Regulation of expression of a cDNA from barley roots encoding a high affinity sulphate transporter. Plant Journal **12**, 875-884.

Speiser A, Silbermann M, Dong YH, Haberland S, Uslu VV, Wang SS, Bangash SAK, Reichelt M, Meyer AJ, Wirtz M, Hell R. 2018. Sulfur Partitioning between Glutathione and Protein Synthesis Determines Plant Growth. Plant Physiology **177**, 927-937.

Suzuki A, Knaff DB. 2005. Glutamate synthase: structural, mechanistic and regulatory properties, and role in the amino acid metabolism. Photosynth Res **83**, 191-217.

Swida-Barteczka A, Krieger-Liszkay A, Bilger W, Voigt U, Hensel G, Szweykowska-Kulinska Z, Krupinska K. 2018. The plastid-nucleus located DNA/RNA binding protein WHIRLY1 regulates microRNA-levels during stress in barley (Hordeum vulgare L.). Rna Biology **15**, 886-891.

Takahashi H. 2019. Sulfate transport systems in plants: functional diversity and molecular mechanisms underlying regulatory coordination. Journal of Experimental Botany **70**, 4075-4087.

Tegeder M, Masclaux-Daubresse C. 2017. Source and sink mechanisms of nitrogen transport and use. New Phytologist **217**, 35-53.

Valot B, Langella O, Nano E, Zivy M. 2011. MassChroQ: A versatile tool for mass spectrometry quantification. Proteomics **11**, 3572-3577.

Vidal EA, Alvarez JM, Araus V, Riveras E, Brooks M, Krouk G, Ruffel S, Lejay L, Crawford N, Coruzzi GM, Gutierrez RA. 2020. Nitrate 2020: Thirty years from transport to signaling networks. Plant Cell. In press

Wang M, Zhao Y, Zhang B. 2015. Efficient Test and Visualization of Multi-Set Intersections. Scientific Reports **5**.

Watanabe M, Balazadeh S, Tohge T, Erban A, Giavalisco P, Kopka J, Mueller-Roeber B, Fernie A, Hoefgen R. 2013. Comprehensive dissection of spatio-temporal metabolic shifts in primary, secondary and lipid metabolism during developmental senescence in Arabidopsis thaliana. Plant Physiology **62**, 1290-1310.

Watanabe M, Hoefgen R. 2019. Sulphur systems biology-making sense of omics data. Journal of Experimental Botany **70**, 4155-4170.

Wawrzynska A, Sirko A. 2014. To control and to be controlled: understanding the Arabidopsis SLIM1 function in sulfur deficiency through comprehensive investigation of the EIL protein family. Frontiers in Plant Science **5**.

Zientara-Rytter K, Lukomska J, Moniuszko G, Gwozdecki R, Surowiecki P, Lewandowska M, Liszewska F, Wawrzynska A, Sirko A. 2011. Identification and functional analysis of Joka2, a tobacco member of the family of selective autophagy cargo receptors. Autophagy **7**, 1145-1158.

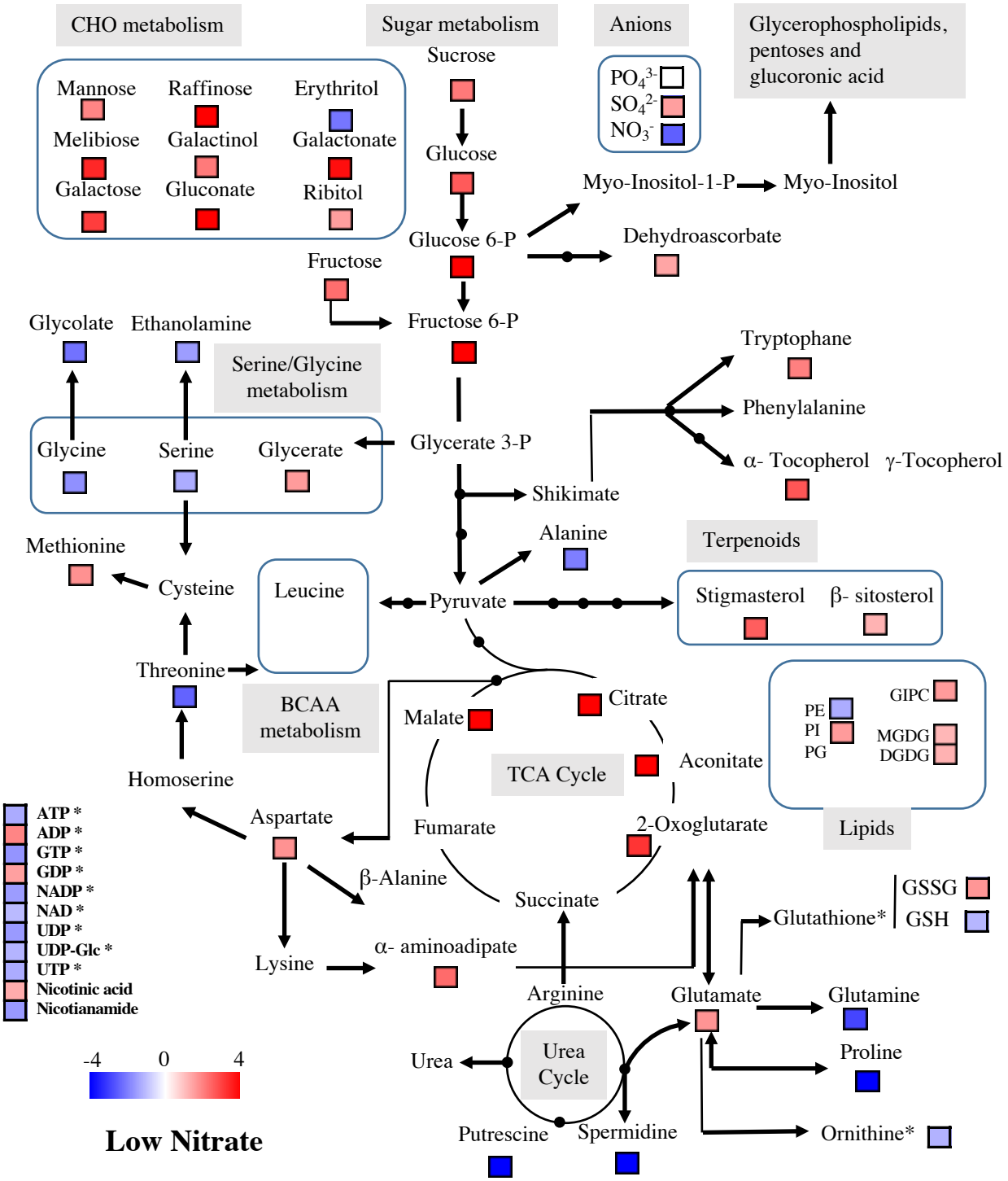

Figure 1: Metabolite changes under low nitrate (Low-N) condition relative to the control (Ctrl) growth condition. The relative metabolite concentrations were measured on the rosettes of plants grown under low nitrate or control conditions for 60 days. Note that when the calculated fold changes (FC) in the Low-N relative to Ctrl condition indicated a decrease (i.e. 0<FC<1), the values were changed to [-1/(calculated FC)] in the figure. Then the FC values ranged between -4 and 4 according to the color code from blue to red. FC are only shown for metabolites significantly different between low N and Ctrl conditions (t-test p-value ≤ 0.05). Negative number means metabolite less abundant in said condition and positive number means metabolite more abundant in said condition. All the metabolites were quantified using GC-MS except those indicated by * that were quantified using LC-MS.

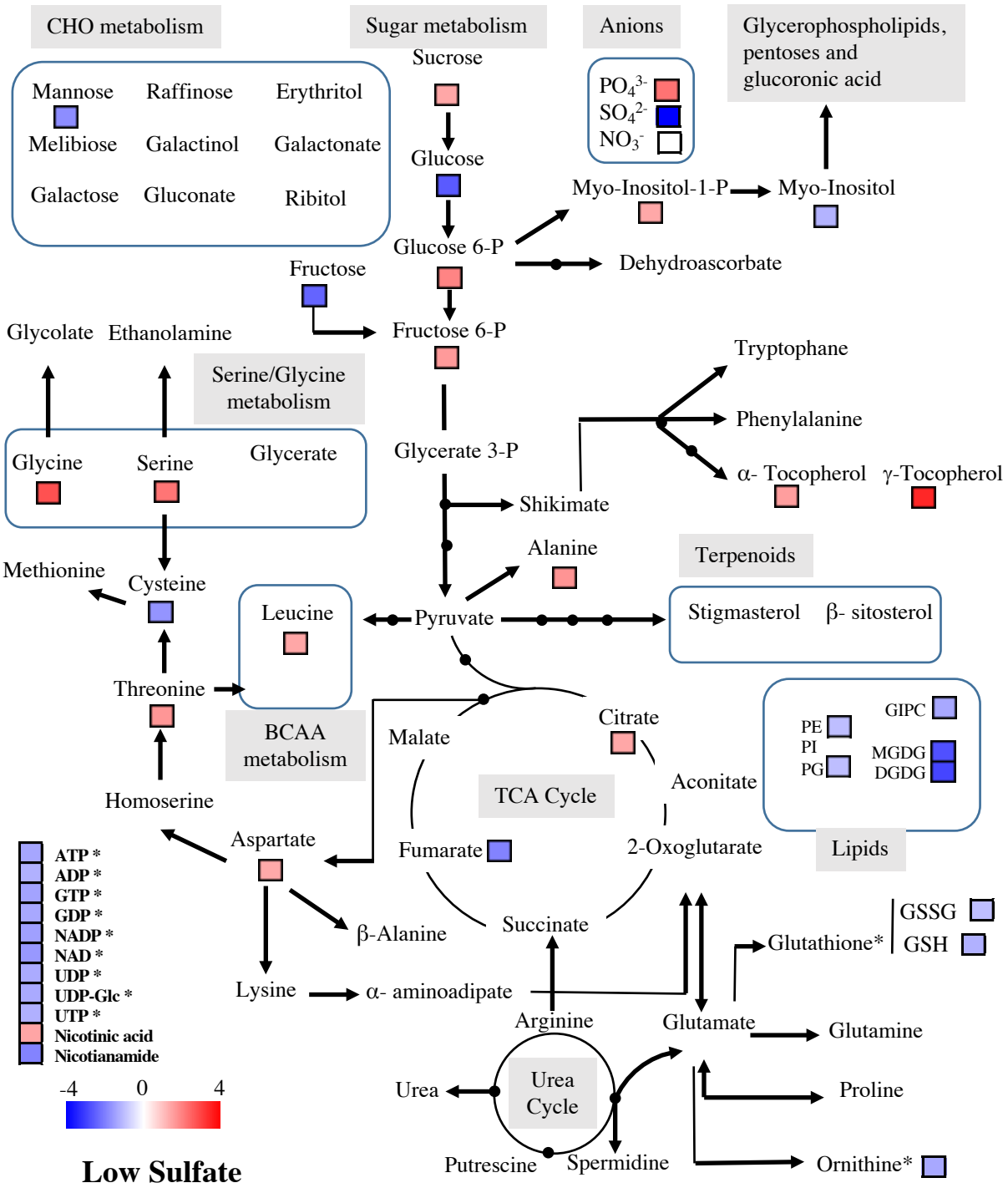

Figure 2. Metabolite changes under low sulfate (Low-S) conditions relative to the control (Ctrl) growth condition. The relative metabolite concentrations were measured on the rosettes of plants grown under low sulfate or control conditions for 60 days. Note that when the calculated fold changes (FC) in the Low-S relative to Ctrl conditions indicated a decrease (i.e. 0<FC<1), the values were changed to [-1/(calculated FC)] in the figure. Then the FC values ranged between -4 and 4 according to the color code from blue to red. Negative number means metabolite less abundant in said condition and positive number means metabolite more abundant in said condition. The same metabolites as in Figure 1 are presented. FC are only shown for metabolites significantly different between low S and Ctrl conditions (t-test p-value ≤ 0.05). All the metabolites were quantified using GC-MS except those indicated by * that were quantified using LC-MS.

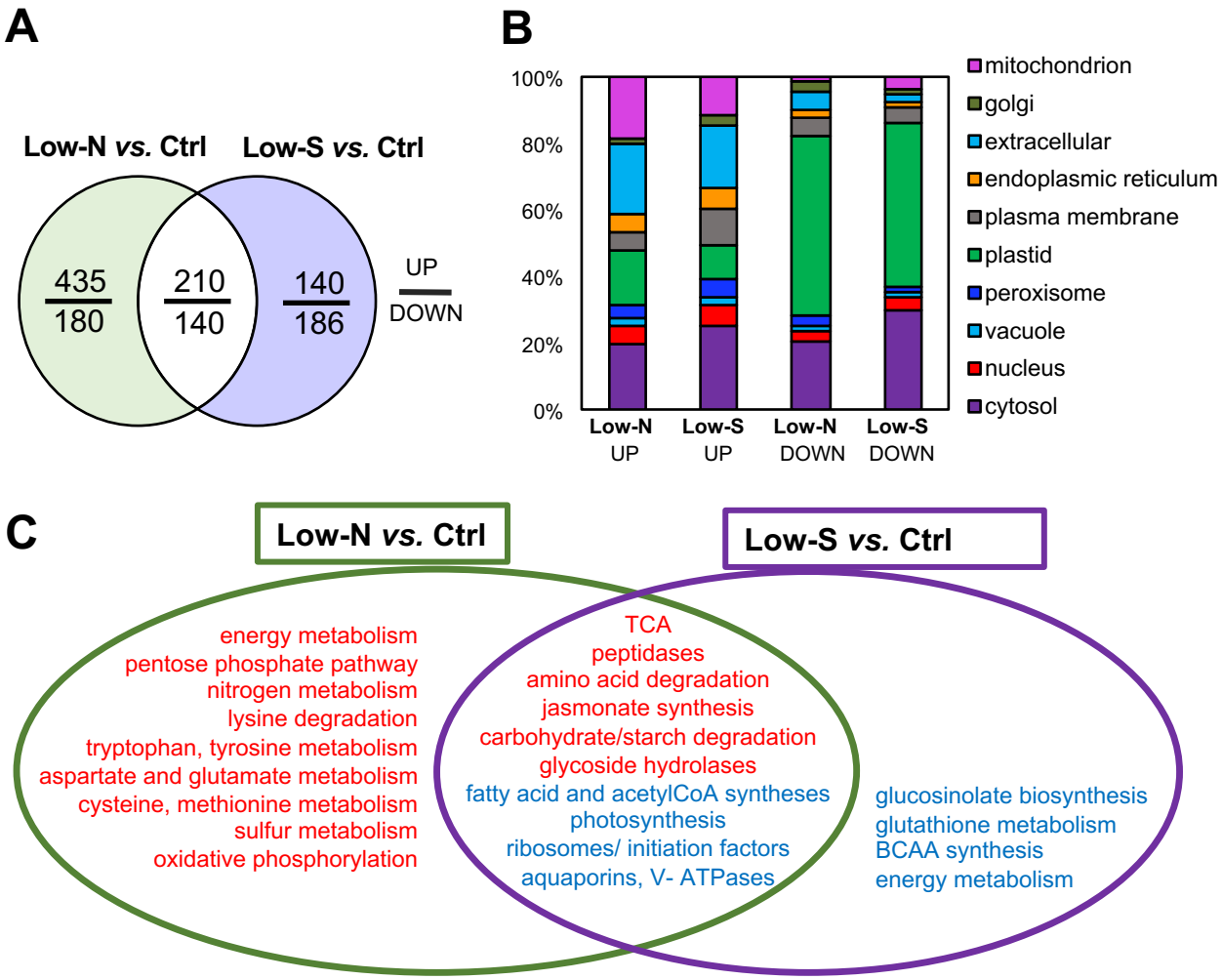

Figure 3: Proteins significantly differentially accumulated (DAPs) under Low-N or Low-S relative to Ctrl. The numbers of up-accumulated (UP) and depleted (DOWN) DAPs under Low-N and Low-S are presented (A). Cellular predicted localisation of DAPs under Low-N or Low-S conditions according to SUBA 4 (B). Significant enrichments of Gene Ontology, Gene Family, AraCyc pathway and KEGG terms for the DAPs accumulated (Red) or less abundant (Blue) under Low-N or Low-S. Significant terms were identified using the VirtualPlant 1.3 BioMaps tool (http://virtualplant.bio.nyu.edu/cgi-bin/vpweb/) applying a P-value cut off of 0.05.

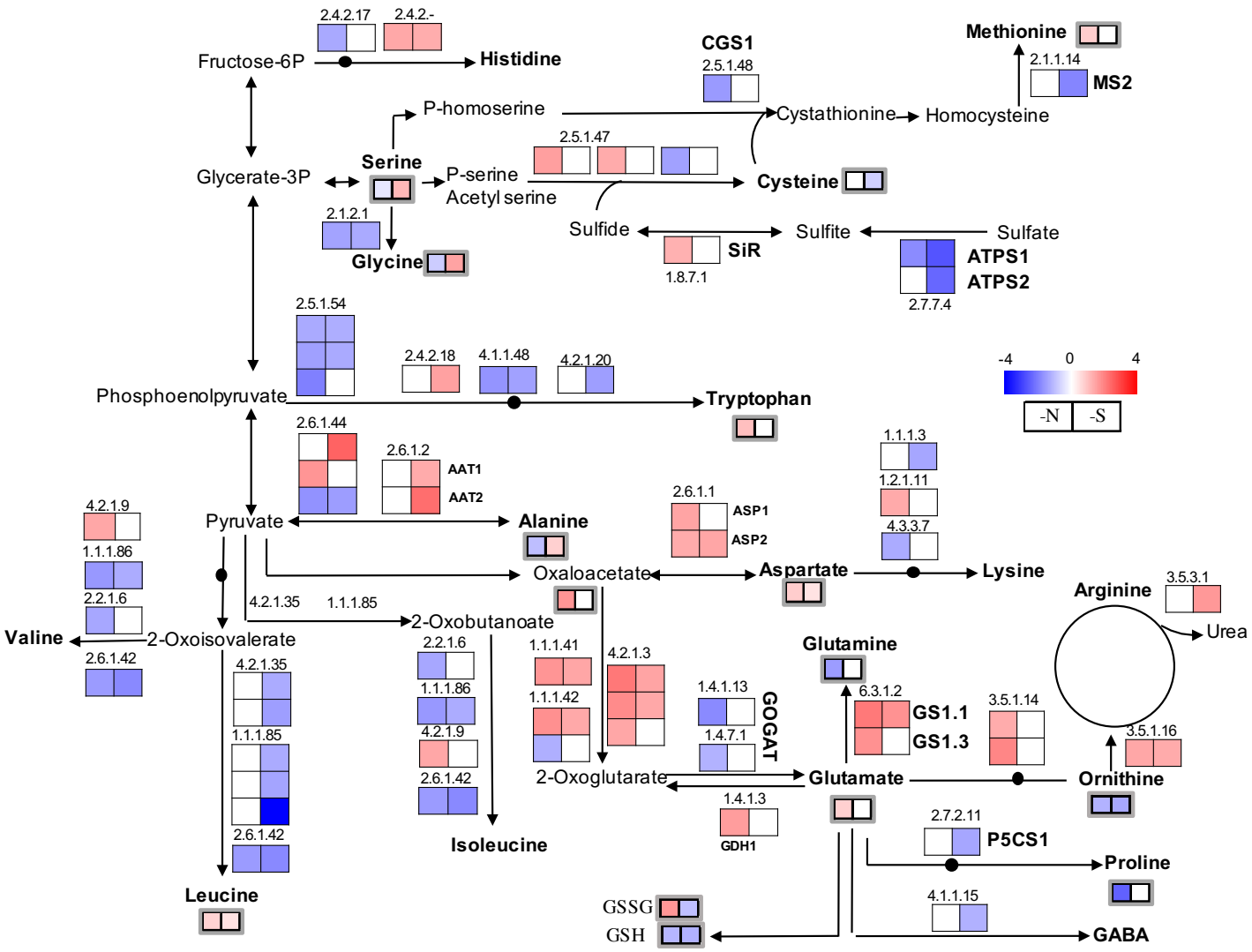

Figure 4: Proteomic changes in amino acid pathway under low nitrate and low sulfate conditions. Significant differentially accumulated proteins (DAPs; big squares; t-test P-value ≤ 0.05) and differentially accumulated metabolites (grey-surrounded small squares) belonging to amino acid metabolism. Fold changes under Low-N (left) and Low-S (right) conditions are shown. Note that like for metabolites in Fig.1 and 2, when the calculated fold changes (FC) in the Low S or Low-N conditions relative to Ctrl conditions indicated a decrease (i.e. 0<FC<1), the values were changed to [-1/(calculated FC)] in the figure. The color codes from blue to red represent fold change values ranging between -4 and 4. Negative number means protein less abundant in said condition and positive number means protein more abundant in said condition. White square indicate non significant changes. Series of four numbers in the figure indicate E.C. enzyme numbers. ASP: aspartate aminotransferase; GDH: glutamate dehydrogenase; GOGAT: glutamate synthase; GS: glutamine synthetase; P5CS1: delta1-pyrroline-5-carboxylate synthetase; GSH: reduced glutathione form; GSSG: oxidized glutathione; SiR: sulfite reductase; ATPS: ATP sulfurylase; CGS1: cystathionine gamma-synthase; MS2: methionine synthase.

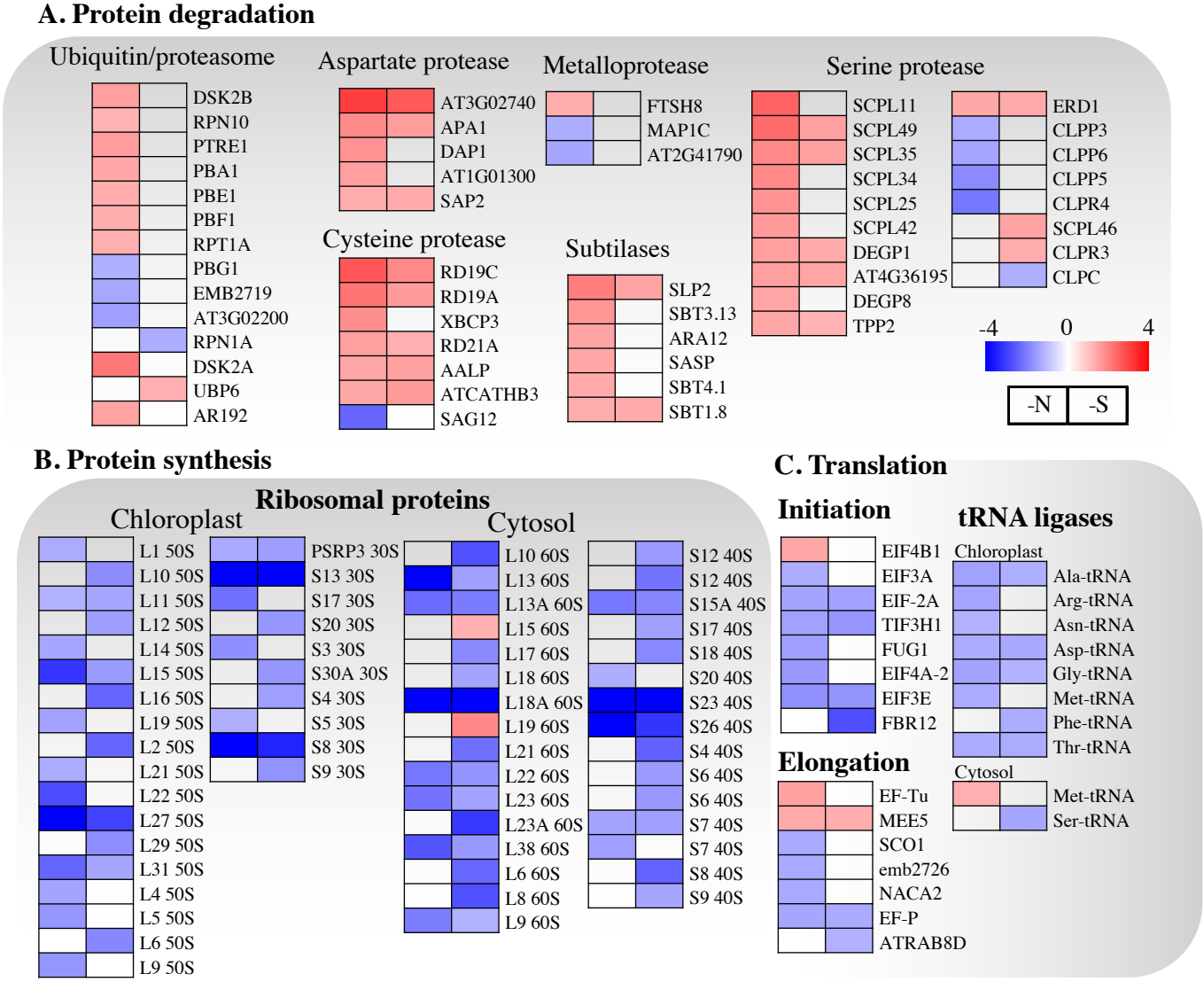

Figure 5: Low nitrate and low sulfate conditions affect protein synthesis and protein degradation in opposite ways. Significant differentially accumulated proteins (DAPs; t-test P-value ≤ 0.05) involved in protein degradation (A) and protein synthesis (B) and translation (C) under Low-N (left) and Low-S (right) conditions. Note that when the calculated fold changes (FC) in the Low-N relative to Ctrl condition indicated a decrease (i.e. 0<FC<1), the values were changed to [-1/(calculated FC)] in the figure. Then the FC values ranged between -4 and 4 according to the color code from blue to red. FC are only shown for proteins significantly different between Low-N or Low-S and Ctrl conditions. Negative number means protein less abundant in said condition and positive number means protein more abundant in said condition. White square indicate non significant changes.

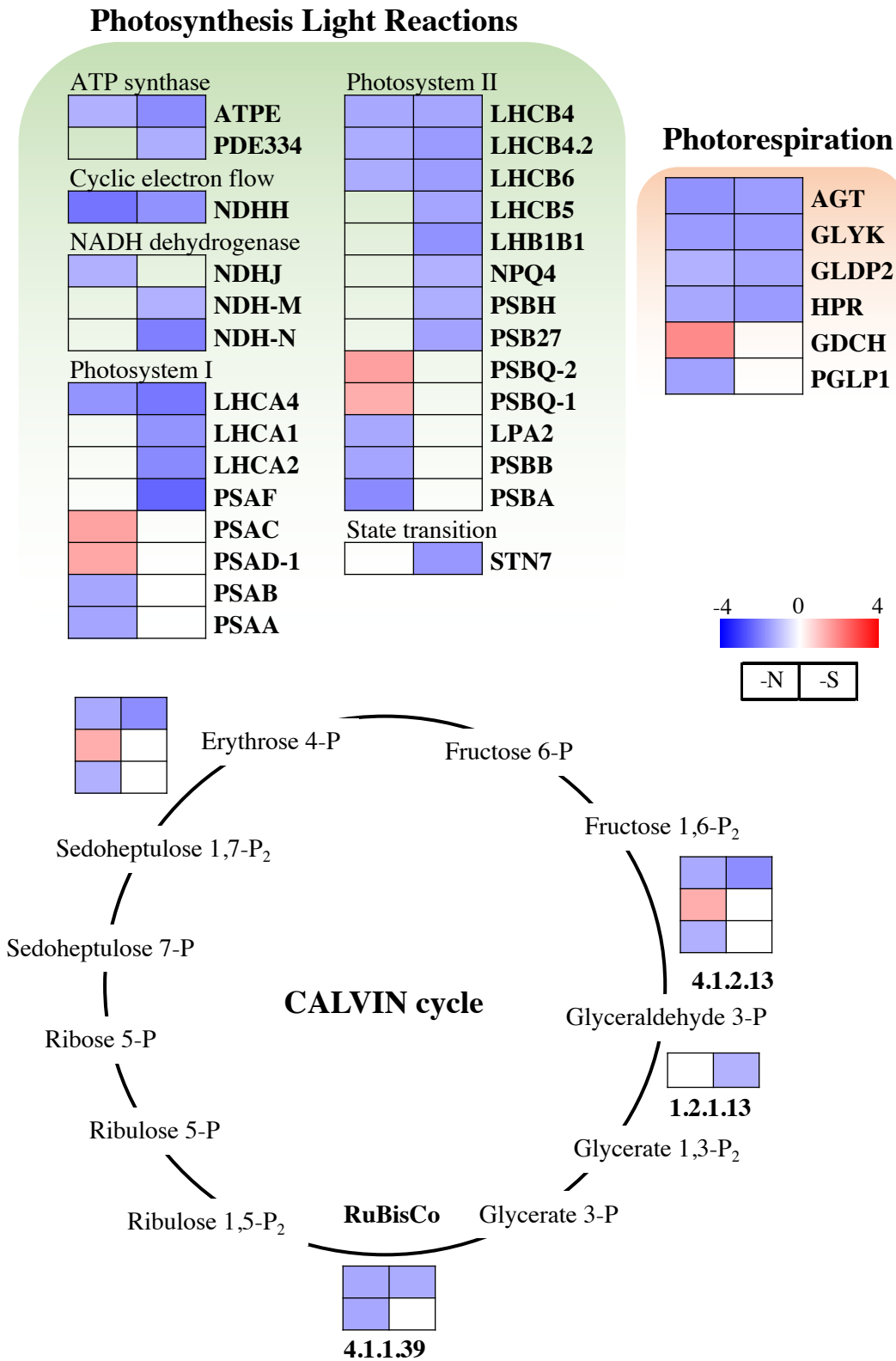

Figure 6: Changes in proteins involved in photosynthesis and photorespiration under low nitrate and low sulfate conditions. Significant differentially accumulated proteins (DAPs; t-test P-value ≤ 0.05) involved in chloroplast carbon fixation and photorespiration under Low-N (left) and Low-S (right) conditions. Note that when the calculated fold changes (FC) in the Low-N relative to Ctrl condition indicated a decrease (i.e. 0<FC<1), the values were changed to [-1/(calculated FC)] in the figure. Then the FC values ranged between -4 and 4 according to the color code from blue to red. FC are only shown for proteins significantly different between Low-N or Low-S and Ctrl conditions. Negative number means protein less abundant in said condition and positive number means protein more abundant in said condition. Series of four numbers in the figure indicate E.C. enzyme numbers. White squares indicate non significant changes.

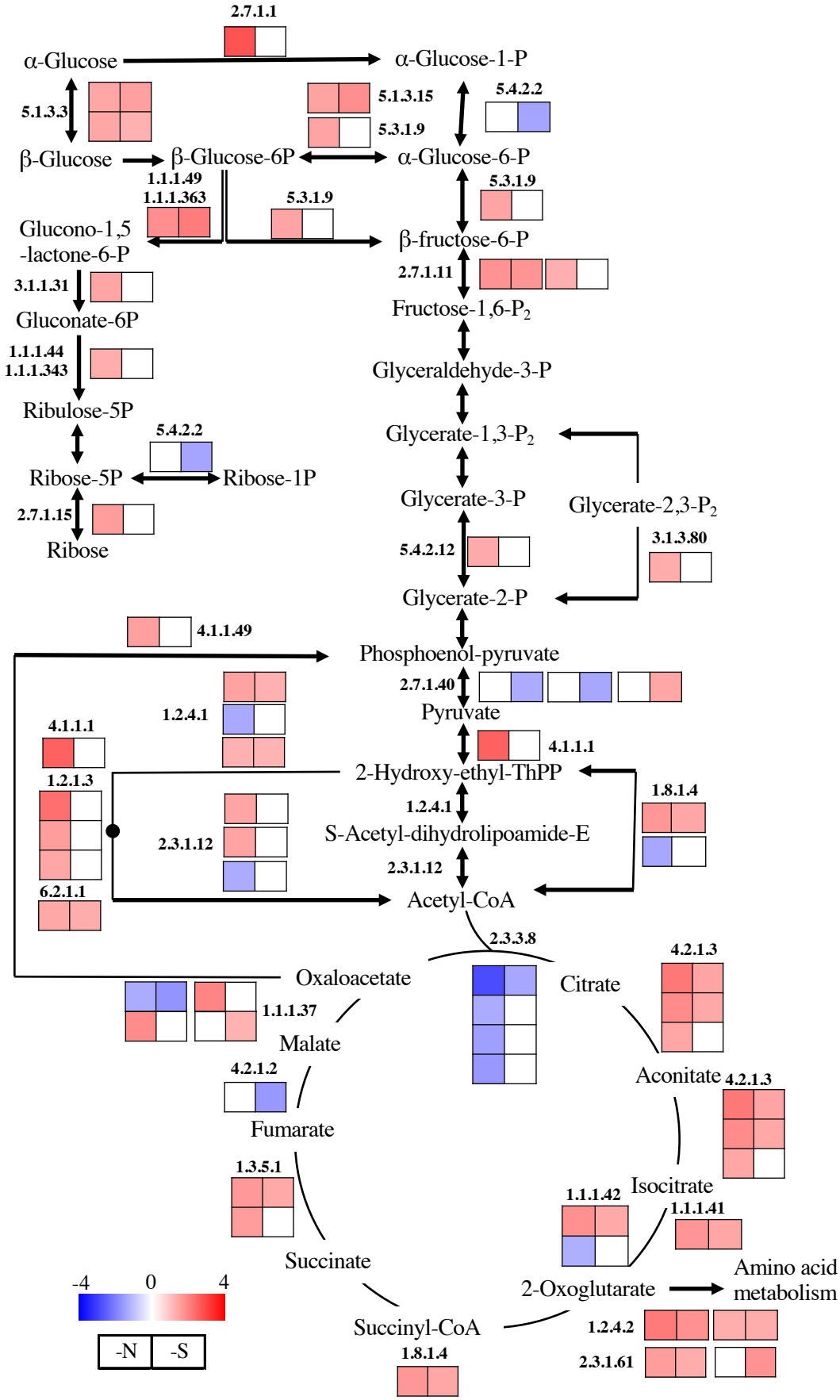

Figure 7: Abundance of proteins involved in glycolysis, TCA cycle and pentose phosphate pathway increased under Low-N and Low-S conditions. Significant differentially accumulated proteins (DAPs; t-test P-value ≤ 0.05) under Low-N (left) and Low-S (right) conditions are shown. Note that when the calculated fold changes (FC) in the Low-N relative to Ctrl condition indicated a decrease (i.e. 0<FC<1), the values were changed to [-1/(calculated FC)] in the figure. Then the FC values ranged between -4 and 4 according to the color code from blue to red. FC are only shown for proteins significantly different between Low-N or Low-S and Ctrl conditions. Negative number means protein less abundant in said condition and positive number means protein more abundant in said condition. Series of four numbers in the figure indicate E.C. enzyme numbers. White squares indicate non significant changes.

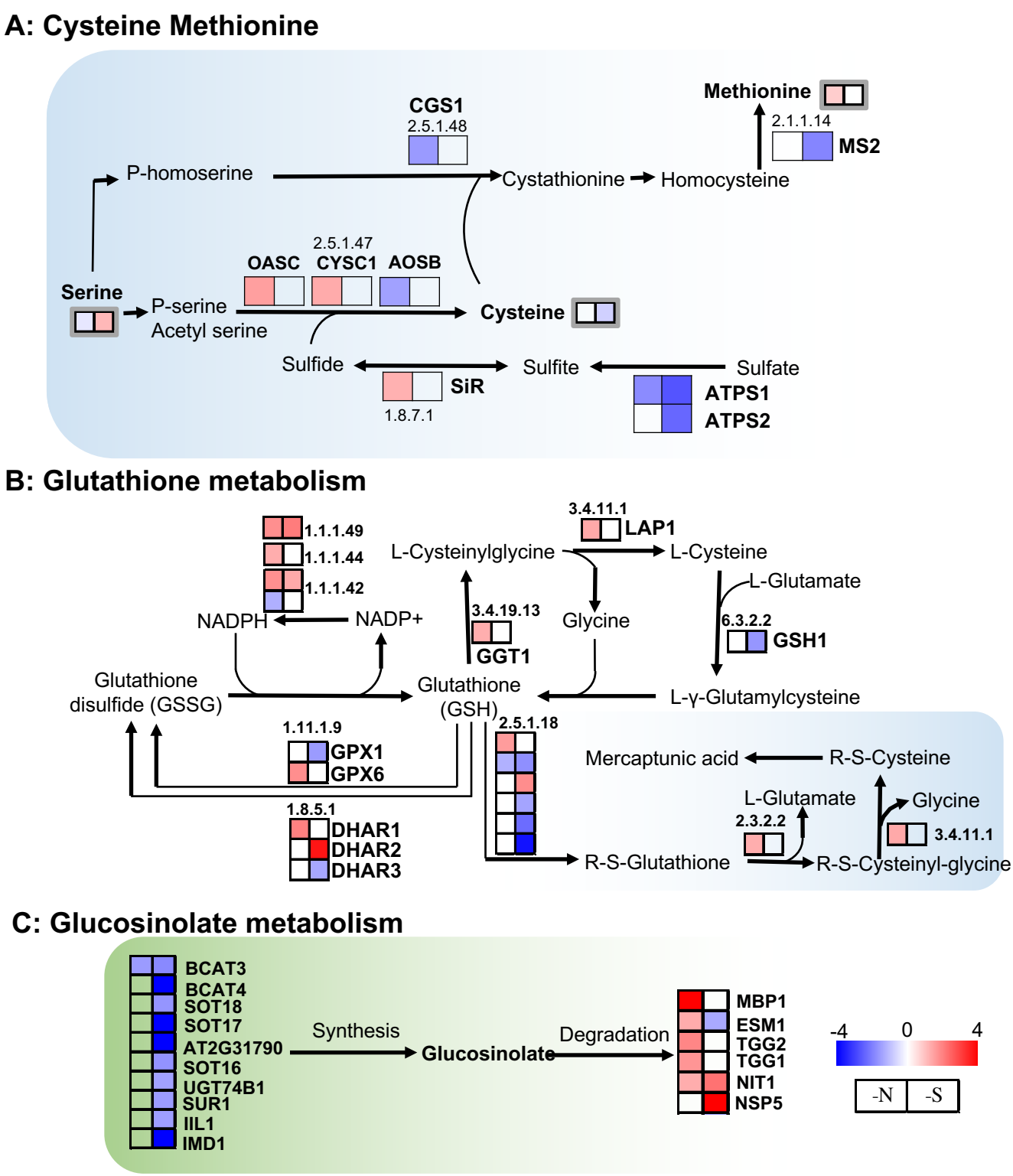

Figure 8: Both low sulfate and low nitrate modify protein content of enzymes involved in sufate assimilation, glutathione and glucosinolate metabolisms. Significant differentially accumulated proteins (DAPs; t-test P-value ≤ 0.05) involved in sufate assimilation (A) glutathione (B) and glucosinolate (C) metabolisms under Low-N (left) and Low-S (right) conditions. Note that when the calculated fold changes (FC) in the Low-N relative to Ctrl condition indicated a decrease (i.e. 0<FC<1), the values were changed to [-1/(calculated FC)] in the figure. Then the FC values ranged between -4 and 4 according to the color code from blue to red. FC are only shown for proteins significantly different between Low-N or Low-S and Ctrl conditions. Negative number means protein less abundant in said condition and positive number means protein more abundant in said condition. Series of four numbers in the figure indicate E.C. enzyme numbers. White squares indicate non significant changes.

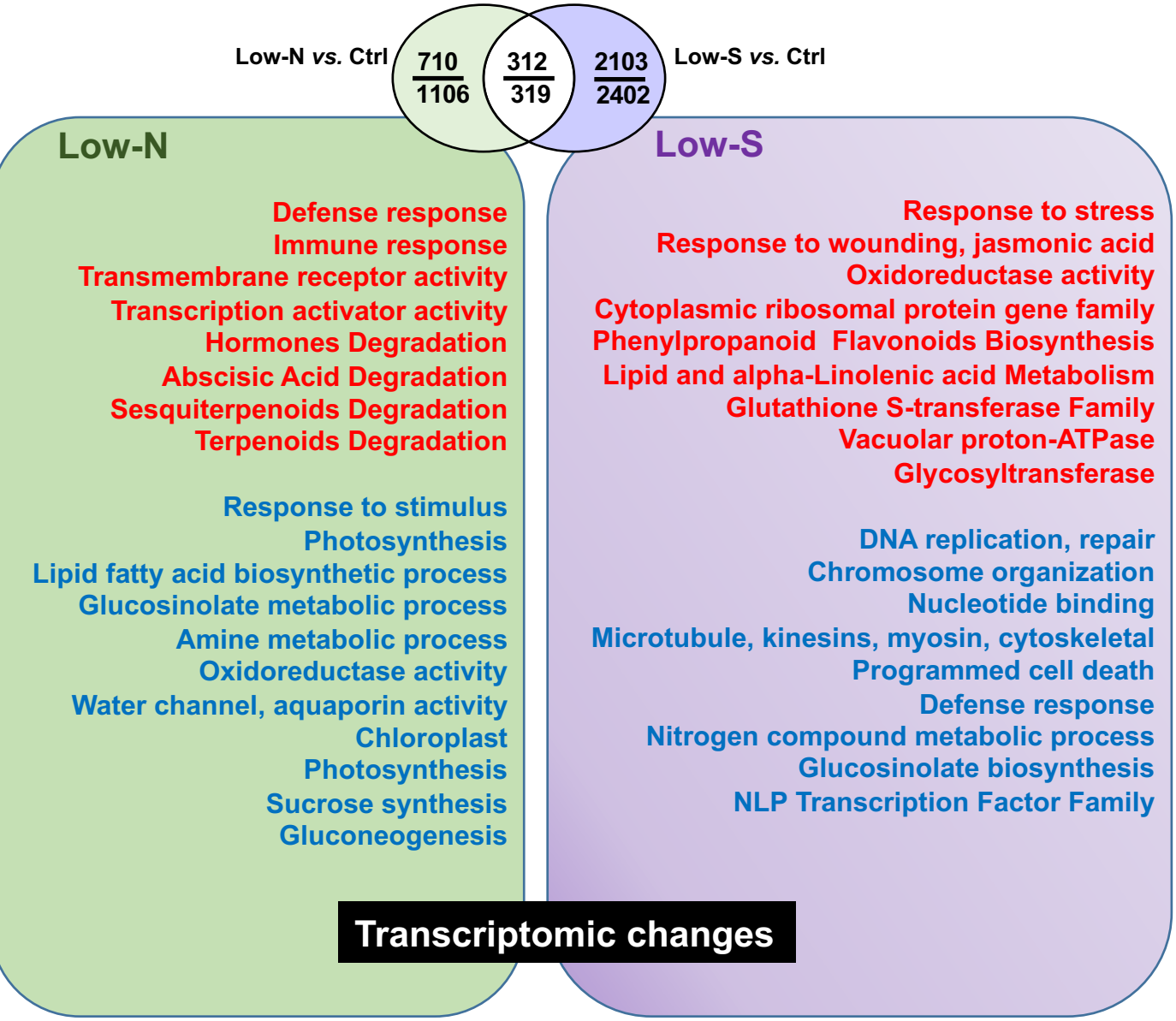

Figure 9: Transcriptomic changes reveal specific effects of Low-N and Low-S conditions. Venn diagram (at the top) presents the number of differentially expressed genes (DEGs) under Low-N, Low-S and in intersection both Low-N and Low-S conditions. The number of up-regulated genes under Low-N or Low-S is indicated above and the number of down-regulated genes below. Significant enrichments in Gene Ontology, Gene Family, AraCyc pathway and KEGG terms for the up-regulated (Red) or dow-regulated (Blue) DEGs under Low-N (left) or Low-S (right) are shown. Significant terms were identified using the VirtualPlant 1.3 BioMaps tool (http://virtualplant.bio.nyu.edu/cgi-bin/vpweb/) applying a *P*-value cut off of at least 0.01 (see Tab.S7 and S8).